

UNIVERSITÀ DEGLI STUDI DI PADOVA

Ph.D. Course Medical Clinical and Experimental Sciences

Curriculum: NEUROSCIENCES

**APPLICATION OF THE ENDOSCOPIC
ENDONASAL APPROACHES TO
VASCULAR NEUROSURGERY:
ANATOMIC AND CLINICAL STUDY.**

Ph.D. STUDENT: ELENA d'AVELLA

TUTOR: PROF. ALESSANDRO MARTINI

Summary

Abstract

1. The exploit of the endoscopic endonasal approaches

1.1 *“All major progress in human evolution occurred in the field of instrument”*- Buckminster Fuller.

1.2 The extended endoscopic endonasal approaches

1.3 The endoscopic endonasal transsphenoidal approach

1.4 The endoscopic endonasal transtuberculum transplanum approach

1.5 The endoscopic endonasal transclival approach

1.6 The endoscopic endonasal approach to the cranio-vertebral junction

2. The (r)evolution of anatomy

3. The application of the endoscopic endonasal approaches to vascular neurosurgery

3.1 Endoscopic endonasal control of the paraclival internal carotid artery by Fogarty balloon catheter inflation

3.2 Endoscopic endonasal surgery for a mesencephalic cavernoma

3.3 The extended endoscopic endonasal transplanum transtuberculum approach to the anterior communicating artery complex: anatomic study.

3.4 Quantitative anatomical analysis of the endoscopic assisted lateral supraorbital approach and endoscopic endonasal transclival approach: two minimally invasive routes to basilar apex aneurysms

3.5 Comparative exposure of the vertebral artery at the cranio-vertebral junction through transcranial and extended endoscopic endonasal approaches

Abstract

Introduction. The expansion of the endoscopic endonasal approach in neurosurgery during the last three decades recently led the neurosurgical clinical interest to the investigation of further application of this technique, namely to neurovascular pathologies. Cadaver dissections studies have represented the milestone in the progressive application of this technique. Integrating anatomical studies with advanced visualization tools and quantification methods increases their impact toward clinical application.

Material and methods. The main endoscopic endonasal approaches were performed and exposure of the vascular intracranial structures was analyzed: the anterior communicating artery complex was investigated through the transplanum transtuberculum approach; the transsphenoidal approach to the sellar area was performed for the exposure of the intracavernous internal carotid artery; the basilar artery was exposed by means of the endoscopic endonasal transclival approach, and the vertebral arteries through the extended endonasal approach to the craniovertebral junction. Possible clinical application of each approach was investigated during anatomical dissections upgraded with imaging and quantification methods.

Results. The transtuberculum transplanum approach allows for the exposure and control of the anterior communicating artery complex; the relationship between the proximal anterior cerebral artery, gyrus rectus, and optic chiasm is the main determinant for the exposure and control of the vessel. Temporary occlusion of the internal carotid artery with a Fogarty balloon catheter through the endoscopic transsphenoidal route might be another maneuver that is useful for obtaining intraoperative control of the vessel. The endoscopic transclival approach may be considered a minimally invasive route to the basilar apex in the presence of specific anatomical and pathological features. Comparative analysis of the anatomical exposure of the vertebro-basilar junction as obtained through transcranial and endoscopic endonasal approaches may be helpful in unlocking this complex skull base area.

Conclusions. The introduction of the endoscopic endonasal approaches for the treatment of cerebrovascular pathologies represents the most advanced and innovative step forward of the skull base endoscopic endonasal surgical technique. The present PhD research activity may add relevant anatomical and clinical information to the rather sparse literature directly focused on surgical indication of the endoscopic endonasal approaches to vascular neurosurgery.

1. The exploit of the endoscopic endonasal approaches

The roots of the endoscopic endonasal approaches derive from a pioneristic contribution of a Korean neurosurgeon working in Pittsburgh, Hae Dog Jho, who presented his early experience about transsphenoidal pituitary surgery in July 1996 at the 6th European Workshop on Pituitary Adenomas (EWPA) in Berlin. He showed through VHS videotape the use of the endoscope instead of the operating microscope as visualizing instrument along the whole endonasal procedure. Encouraged by the visualization provided by endoscopes during surgery for inflammatory disease of the sphenoid sinus, Jho and colleagues decided to explore the potential use of endoscopic techniques in pituitary surgery (1-3).

Except for the use of the operating microscope, advocated and popularized by Hardy at the beginning of the 1980s, the transsphenoidal approach had changed little over the years since its introduction by Schloffer (1907), Hirsch (1909) and finally Cushing (1910), either through the sublabial or septal incision. In brief this technique requires a wide elevation of the mucosa of the floor of the nose and septum, and resection of the osseous septum and rostrum of the sphenoid sinus to reach the sella turcica. Resection of the pituitary tumor is then performed under microscope magnification and intraoperative fluoroscopic imaging. The visualization provided by the operating microscope is limited by the optical properties of the lens and the light source. With the microscope, illumination and the angle of the visual field are restricted. Consequently, despite magnification, injuries to the carotid artery and optic nerves, although uncommon, still represent potential catastrophic complications during transsphenoidal pituitary surgery. Postoperatively, the patient is afflicted with facial swelling and often requires nasal packing. Complications such as sinusitis, nasal synechiae, septal perforation, and numbness of the upper incisors are common (4-7). In 1994, Cooke and Jones reported the use of the endonasal route to the sella in 48 patients with pituitary lesions, as a straightforward and quick approach that does not require dissection of nasal mucosa or removal of septal cartilage. They achieved successful access to the pituitary fossa with no nasal, septal, dental, or sinus complications (8).

With his contribution, Jho standardized the surgical technique for the transnasal transsphenoidal endoscopic approach, highlighting its multifold advantages. In terms of surgical trauma, since the patient does not require sublabial or nasal incision and mucosal dissection from the nasal septum, potential oro-nasal complication are eliminated; in most

cases postoperative obstructive nasal packing is not necessary and patients can have free nasal airway. Regarding the optical properties of the endoscope, it provides a panoramic view of the sphenoid sinus and has a focal length that ranges from 1 mm away from the object to infinite. In contrast to the limited visualization of the anterior wall of the sella offered by the microscope, the endoscope provides an exquisite view of the main anatomical landmarks, which may minimize the chance of catastrophic injury of the carotid artery. Certainly, there is a learning curve for the surgeon who is not familiar with endoscopic technique. Endoscopic and microsurgical techniques require different surgical skills. With the procedure performed through one nostril, the endoscope and surgical instruments need to be carried in parallel to each other, with the endoscope usually held by the non-dominant hand and the surgical instruments by the dominant hand. An inexperienced surgeon will encounter frustration when the two instruments displace each other in the small surgical field. In addition, the monocular vision of the endoscope does not provide depth perception, which may be initially disconcerting for the surgeon accustomed to the binocular view provided by the operating microscope (2,9-10).

The premonitory intuition of Jho and colleagues that in the future the application of endoscopes in neurosurgery would be expanded by refinements in technology, dedicated instruments and improved imaging quality proved to be correct. During the last three decades, endonasal endoscopic surgery has become the method of choice for the treatment of the pathologies of the sellar region, and also for lesions that originate or extend into the regions around the sella (11-14).

1.1 “*All major progress in human evolution occurred in the field of instrument*”- Buckminster Fuller.

The evolution from the microsurgical transsphenoidal trans-rhino-septal approach to the “pure” endoscopic endonasal transsphenoidal one developed gradually, concurring with increasing familiarity with the view of the nasal and sphenoid anatomical structures, and improvement in video instrumentation and surgical instruments.

The video-instrumentation system may be artificially divided into four main parts: the generator of the light (light source); the transmission of the light (endoscope and cable); the image acquisition (camera); the image displayer (video monitor). Concerning the light source, even though several types are currently available (mainly halogen and xenon), it is better to use cold xenon light sources, which determine lower heat dispersion with a

subsequent reduced risk of damage to the neurovascular structures. Furthermore, the xenon light source has a color temperature of 6,000 K, the same as solar light; it is as if we were using the sun to light the operating field, with a chromatic return similar to reality. The endoscope employed must be a rigid one, 4 mm in diameter, 18–30 cm in length, and with 0°, 30°, 45° lenses, according to the different steps of the operation. The endoscope must be introduced into a shaft, connected to a cleaning/irrigation system controlled by a manual or foot switch. The irrigation system permits the distal lens to be cleaned, thus avoiding repeated entrances and exits from the nostril. The use of an 18-cm, 0° endoscope is advised during the nasal and sphenoid steps of the operation, because it is easier to handle. The use of angled endoscopes (30° and 45°) is advised in the sellar phase of the procedure, to explore the residual cavity, after lesion removal, or to inspect the suprasellar and parasellar compartments. The endoscope is connected to a cable, made up of a bundle of optical fibers that must be handled carefully to avoid twisting them. The camera connected to the endoscope should be fitted with 3CCD sensors. These sensors are electronic systems, which transform the real image (photons) into electronic images, visible on the screen. The 3CCD camera offers significantly enhanced sharpness and contrast of the video images compared with the mono CCD camera, because each of the sensors processes one of the primary colors of the image separately. Furthermore, the visual acuity is significantly better using the 3CCD camera compared with the mono CCD. The 3CCD camera has to be combined with a 2100 monitor, supporting the high resolution of the 3CCD camera. The high-resolution monitor has a horizontal resolution of >750 lines. Since the resolution of the 3CCD digital camera is superior to 750 lines, if a monitor with a lower resolution is used, some of the sharpness of the endoscopic images is lost. Finally, in order to guarantee a suitable file of surgical images, the use of a digital video recorder system (DV-CAM), which gives superior quality and lasting images, or a direct acquisition system on hard disk in DV “broadcasting” format or on DVD-R RW are recommended. Despite the fact that the quality of endoscopic imaging reached an incredible high-quality standard only 20 years ago, one of the main limitations to its widespread use in neurosurgery still stems from drawbacks due to handling of the endoscope, cumbersomeness related to the camera and light cable connections, and maneuverability inside the skull. Different fiberscopes and rigid endoscopes have been proposed with smaller diameters and shorter lengths, including the latest videoendoscopes with the “chip stick” technology. However, the downside of optimizing miniaturization and weight reduction has always been deterioration of the quality of vision. Unfortunately, in an era where high definition (HD) quality images are the standard and dominate both the

endoscopic and microsurgical fields, inadequate image quality is no longer tolerable. According to these strict requirements, above all the need to couple miniaturization and high image quality, new videoendoscopes equipped with an HD chip were recently developed (15-19). The endoscope provides a bi-dimensional view and the image as seen on the monitor is the result of a computer elaboration process; loss of spatial and depth information, however, can be overcome with developing experience of the surgeon and also because of the capability of the human brain to elaborate secondary spatial depth cues, e.g., shadows, lights, and parallax movements. The introduction and evolution of three-dimensional (3D) technology in endoscopic surgery has been claimed as a viable solution to overcome limits of two-dimensional vision, although it has not yet become widespread. Current “3D” technology is not strictly 3D, because it provides a complex recombination of two frames of images captured from different angles and requires the use of dedicated glasses to fuse these into a single image. New generation 2D instruments, featuring Ultra-HD (UHD) technology, do not have these requirements. One claimed advantage of 3D endoscopic surgery is improvement in “hand-eye” coordination, with a better understanding of tissue characteristics and anatomy. This is of particular relevance for novice surgeons, because anatomic details and depth perception gained with 3D endoscopes allow the naive operator to train with faster and better results. When one performs the initial step of endoscopic endonasal surgery, the benefits of 3D endoscopes are of little significance, because of the narrow space represented by the nasal fossae. On the other hand, increased depth perception is achieved during the intrasellar and, mostly, the intradural parts of surgery. Advantages with the use of 3D technology also are evident in the reconstructive step (20-24).

Concerning the surgical instruments, it must be kept in mind that the endoscopic endonasal access for the surgical tools through the nostril is narrower than that of the microsurgical procedure, since working room is given by the nostril and not by the nostril widened by the nasal speculum. But, on the contrary, the maneuvering angle is much wider, and not conditioned by the nasal speculum. Moreover, so that the neurosurgeon can work with both hands, as he is accustomed to doing, the adoption of a table-mounted endoscope holder is useful, of which many different versions exist, either purely mechanical or pneumatic. From the time when the instruments used in the microsurgical approach were of a bayonet shape, due to the requirement of not rendering visible the surgeon’s hands in the operating field (a conflict between the surgeon’s hands and the lens of the microscope), and the lens of the microscope being far from the surgical field, with the endoscopic endonasal technique we switched to straight instruments that slide along the endoscope, whose lens is

now near to the surgical target. Dedicated instruments for the endoscopic approach have been realized in order to: move easily and safely in the nasal-sinusal, sellar and skull base regions; provide safe handling and grasping, avoiding the conflict between the surgeon's hands and the endoscope; be well balanced and ergonomic; allow easy reaching of every visible zone of the surgical field, both using 0° and, above all, angled optics. The "ideal" instruments have not yet been conceived and further development is expected (25-26).

Investigation of materials and tissues used in the endoscopic endonasal approaches has tremendously contributed to the expansion of clinical application of this technique. The endoscopic approaches all share the need of a laborious reconstruction phase to prevent the risk of cerebrospinal fluid leak. With the use of dural substitutes and sealants, together with autologous graft material and pedicled vascular flap, the rate of post-operative cerebrospinal fluid leak has decreased to around 5 % (27-31).

1.2 The extended endoscopic endonasal approaches

The following step, with the inspection of the areas involved in the so called extended approaches, was possible thanks to the huge scientific and surgical activity performed at the University of Pittsburgh (USA), where the group of neurosurgeons and otorhinolaryngologists led by Amin Kassam offered the key in the next years to develop new strategies on pathologies, such as craniopharyngiomas, anterior skull base meningiomas and chordomas, which were not usually considered previously amenable to transsphenoidal surgery (32-36). Acquaintance with endoscopic endonasal anatomical perspective and surgical technique allowed to understand in detail and feel confident expanding the skull base exposure via the endoscopic endonasal perspective beyond the sella, along the whole midline skull base from the crista galli to the cranio-vertebral junction, and its lateral limits. In contrast with the standard endoscopic approach, in which the sphenoid sinus provides the surgical space to gain access to the sellar region, the extended approaches require the creation of a wider surgical corridor to expose and work in different areas beyond the sella. The creation of such surgical corridors includes removal of nasal and paranasal structures, i.e. middle turbinates, posterior portion of the nasal septum, anterior and posterior ethmoid cells, in order to allow the use of two or three instruments, in addition to the endoscope, through both nostrils. On the other hand, different routes and trajectories through the paranasal sinuses are explored, beside the one offered by the sphenoid sinus to the middle skull base (37-46).

1.3 Endoscopic endonasal transsphenoidal approach

In most cases the operation can be done through one nostril. The decision as to which nostril to use for the surgery is made on the basis of the width of the nasal cavity and the laterality of the tumor. The nose is decongested using surgical cottonoids moistened with decongestant solution. During the standard endoscopic transsphenoidal approach to the sella no nasal structure is usually removed; instead many of them must be recognized in order to perform a safe anterior sphenoidotomy and reduce complications related to the nasal phase of the approach. After the introduction of the endoscope inside the nasal cavity, the first visible structures are the inferior turbinate, on the lateral side, the nasal septum, on the medial aspect, and the choana inferiorly. Further advancement of the endoscope identifies the middle turbinate, which is pushed laterally in order to create the passage for the endoscope up to the sphenoid ostium. This is located behind the tail of the superior turbinate, almost 1,5 cm above the roof of the choana. Here the posterior portion of the nasal septum is detached from the sphenoid rostrum, the whole anterior wall of the sphenoidal sinus is enlarged circumferentially, taking care not to enlarge the sphenoidotomy too much in the infero-lateral direction, where the sphenopalatine artery and its major branches lie, and the sphenoid sinus is entered. Sphenoid sinus shows variations in size, pneumatization and septa. In the majority of cases, a large septum separates the sphenoid sinus in two sides and smaller septa divide each side in multiple smaller cavities. The septa are removed allowing a better inspection of the posterior wall of the sphenoid sinus. Many landmarks are recognizable: the sellar floor in the center, the sphenoid planum above and the clival indentation below, the bony prominences of the internal carotid arteries and of the optic nerves laterally on both sides, and between them is the opto-carotid recess, molded by the pneumatization of the optic strut of the anterior clinoid process. The protuberance of the internal carotid artery can be divided into two segments: the paraclival internal carotid artery, which is lateral to the clival indentation, and the “shrimp-” or C-shaped parasellar internal carotid artery, which is lateral to the sella. The anatomical landmarks on the posterior wall of the sphenoid sinus are better visualized and give a better orientation in well-pneumatized sphenoid sinus. A small fenestra is opened with a microdrill or a bone curette on the anterior wall of the sella. The dura mater is opened with a cruciate incision using a sickle blade or angled microscissors. Under direct endoscopic visualization, the tumor is removed using microsuction and pituitary curettes, with preservation of the normal pituitary gland tissue. Resection of larger tumors with

extrasellar extension requires the identification of the arachnoid membrane. With the insertion of the endoscope into the sella, it is possible to follow the extrasellar extension of the tumor and to preserve the diaphragm sellae. In contrast, the operating microscope does not allow direct visualization of the intrasellar tumor. Using the endoscope, the surgeon can better distinguish between tumor and normal pituitary gland tissue (47-49).

1.4 Endoscopic endonasal transtuberculum transplanum approach

This approach allows for access to the suprasellar region and the sphenoid planum, through a more anterior trajectory compared with the one used to reach the sellar region. This route requires a wider opening of the anterior wall of the sphenoidal sinus, which is obtained by removing the superior (supreme) turbinates and the posterior ethmoid air cells located laterally to these turbinates. In the course of such maneuvers, particular attention must be paid to avoid damaging the posterior ethmoidal artery, a branch of the ophthalmic artery that passes through a thin osseous channel along the roof of the ethmoid. It is also important not to extend the removal of the nasal septum and the ethmoid too anteriorly, to avoid damaging the olfactory nerve endings or the cribriform plate of the ethmoid. Once the sphenoid cavity is completely exposed, all of the septa inside it have to be removed up to their attachment to the planum or to osseous prominences such as the optic or carotid prominences. This provides a very wide exposure of the entire sphenoid cavity. Lateral septa often lead directly to the ipsilateral optico-carotid recess, providing an excellent anatomical guide as well as some potential for damage to the associated critical structures. Above the sellar floor, the angle formed by the convergence of the sphenoid planum with the sellar floor is recognized; from the intracranial view, this corresponds to the tuberculum sellae. As one moves the endoscope in an anterior direction, the sphenoid planum is visible, laterally delineated by the protuberances of the optic nerves that diverge toward the apices of the orbits. The opening of the planum starts with the removal of the tuberculum sellae, extended bilaterally in the direction of the optico-carotid recesses. The upper half of the sellar floor and the posterior portion of the planum sphenoidale are removed first, isolating the tuberculum. Once this has been done, the thinned tuberculum is carefully fractured and dissected from the dura mater, being careful to avoid entering the superior intercavernous sinus. The removal of the tuberculum sellae and/or the sphenoid planum is extended in a postero-anterior direction for 1.5 to 2 cm, but not beyond the posterior ethmoidal arteries. The lateral extension of the opening is limited by the protuberances of the optic nerves. Next, the dura mater above the

pituitary gland is opened, allowing visualization of the intracranial structures. The chiasm and the optic nerves are clearly visible. We can consider two endoscopic surgical corridors, one below the chiasm and one above it. Below the chiasm, the pituitary stalk and gland with their vascular supply are visible. Passing the scope between the pituitary stalk and the supraclinoid portion of the internal carotid artery, the ventral surface of the chiasm, the optic tract, and the proximal portion of the anterior cerebral artery are all visible. After opening the Liliequist membrane by directing the endoscope over the dorsum sellae, it is possible to reach the posterior cranial fossa and to expose the upper portion of the brainstem. The basilar artery apex, posterior cerebral arteries, and superior cerebellar arteries, with the third cranial nerves between them, are clearly exposed. By angling the endoscope above the chiasm after the lateral displacement of the medial surfaces of the frontal lobes, the anterior part of the circle of Willis is visible (50-54).

1.5 Endoscopic endonasal transclival approach

The endoscopic endonasal approach to the clivus represents an increasingly important surgical corridor for skull base surgery. It provides surgical access to the ventral midline skull base of the middle and posterior fossa. Access to the clivus is achieved via a more caudal trajectory than is necessary for access to the sellar region. Along such a trajectory, the vomer and the inferior wall (floor) of the sphenoidal sinus are found. Depending on its degree of pneumatization, the sphenoid floor will divide the sphenoid portion of the clivus from the rhinopharyngeal segment, in variable proportions. Entry into the posterior cranial fossa through the clivus is most easily gained in patients with a retrosellar-type sphenoidal sinus. In these cases, the clivus is thinner than in patients with a conchal-type structure. The preliminary steps of the procedure include the previously described middle turbinectomy on the side of the approach (usually the right), wide anterior sphenoidotomy with removal of all septa, and removal of the posterior portion of the nasal septum to allow a binasal approach. The nasal mucosa is detached from the vomer and along the inferior wall (floor) of the sphenoidal sinus. The mucosa is dissected laterally until the vidian nerves are identified; this represents the lateral limits of the surgical corridor. The vomer is completely removed and the bone of the clivus is drilled. Exposure is limited superiorly by the pituitary gland, laterally by the paraclival internal carotid artery and inferiorly by the inferior wall of the sphenoid sinus. The clivus contains the basilar plexus, which is the most extensive series of intercavernous venous connections across the midline. The superior and inferior petrosal sinuses join the basilar plexus. The abducent nerve enters the cavernous sinus by passing through the basilar

sinus close to the paraclival tract of the internal carotid artery; therefore, particular attention should be paid during bone removal in this already complicated area. The dorsal meningeal artery, a branch of the meningohypophyseal artery, provides the arterial blood supply to the dura mater of the clival region, and its course is in proximity to that of the abducent nerve. Dural opening is performed, with particular attention to the sixth cranial nerve, which passes just medially to the carotid artery. The basilar artery, its branches and the ventral surface of the brainstem are visualized (55-58).

1.6 Endoscopic endonasal approach to the cranio-vertebral junction

This approach can be considered the extreme inferior extension of the previously described endoscopic approach to the clivus. The first steps of the procedure are in fact the same as for the endoscopic approach to the clivus. The middle turbinectomy, the removal of the posterior portion of the nasal septum, the wide sphenoidotomy up to the identification of the vidian nerves and the removal of the vomer and the inferior wall/floor of the sphenoidal sinus are performed in the same manner as in the extended endoscopic approach to the clivus. The main difference consists of the complete removal of the vomer, extending inferiorly, down to the hard palate. This is done to allow the widest exposure of the rhinopharynx and to avoid any conflict among the instruments during the next surgical steps. The lower third of the clivus is removed out to the occipital condyles, and the foramen lacerum on both sides is identified because it represents the lateral limit of the approach. Once a wide surgical corridor has been created, the mucosa of the rhinopharynx is removed and the atlanto-occipital membrane, longus capitis and longus colli muscles, and the anterior atlas and axis are exposed. The anterior arch of the atlas is removed, the dens is exposed, and it is thinned using the microdrill. The dens is then separated from the apical and alar ligaments, dissected from the transverse ligament, and finally removed. At this point, a wide surgical corridor allowing access to the anterior portion of the foramen magnum has been created. After the opening of the dura mater, all the neurovascular structures running through the anterior part of the foramen magnum can be visualized. The vertebral arteries can be explored from their entrance in the vertebral canal up to the vertebral artery. The two branches of the intradural segment of the ventral artery (the posterior inferior cerebellar artery and the anterior/ventral spinal artery) are visible as well. The hypoglossal nerve can be identified behind the first tract of the intradural vertebral artery. This nerve arises along the front of the inferior olive as a series of rootlets that converge on the dural orifice of the hypoglossal canal. Below the entrance of the vertebral artery, the dentate ligament and the ventral rootlets of the first and

second spinal nerves can be visualized in the spinal canal. Passing the endoscope superior and posterior to the vertebral artery, the lower cranial nerves and the acoustic–facial bundle (seventh and eighth cranial nerves) are explored along with the anterior inferior cerebellar artery (58-63).

2. The (r)evolution of anatomy

Laboratory exercise and anatomical dissections are the best ways to achieve both anatomical knowledge and surgical technique, with a unique haptic confidence and feedback. In particular, cadaveric anatomical dissections allow exploration of delicate and surgically forbidden regions, giving the “beginner” the chance to truly visualize and memorize the complex anatomical structures and their relationships, and the experienced surgeons the possibility to improve their technical skills (64-69). Anyway, human cadaver models have the main disadvantage of lack of reproducibility of some physiopathological conditions that rule surgery. Starting from preparation of the cadaver specimens, maintenance of the real consistency of brain parenchyma and physiological relationship with neurovascular structure is extremely difficult, both with freezing and fixation techniques. Many attempts have been done in the set of anatomical laboratories to reproduce physiological hemodynamic factors. However, the vast majority of models have focused on performing surgical approaches in the setting of normal surgical anatomy, without the chance of reproducing neither arterial and venous bleeding, hemostasis control, nor circulation of cerebrospinal fluid in the subarachnoid cisterns. The anatomy distorted by a space-occupying lesion and the skills required for dissecting a tumor from the surrounding neural and vascular structures are other factors that may limit the application of anatomical training to real surgery (70-74).

With the limitations first exposed, dissection lab experience teaches thinking about anatomy as the basic method to understand anatomy and as a crossroad to develop anatomic scientific projects, a source of inspiration of new ideas, since anatomy is not merely concerned with the description of structures. Rather, it is a science in evolution devoted to clinical and surgical advances and the beauty of the “art” of anatomy may not be separable from its application in a surgical milieu (64).

Coming to the endoscopic endonasal approaches, cadaver dissection studies have represented the milestone in the learning curve toward gaining confidence with a different and somehow distorted anatomical perspective compared with the one provided by the transcranial approaches. They allowed us to fix the anatomical landmarks, overcome the

initially reduced ability for the endoscope maneuverability, improve eye-hand coordination, and not to lose orientation in the vision offered by the endoscope on the video monitor, with a different sense of depth compared with that gained with the microscope (32,47,49).

Entrance of a mathematic attitude in the field of cadaver dissection studies added new fuel to anatomical research, changing the paradigm for the analysis of surgical anatomy itself: from a static point of view (anatomical dissection to display and measure a given approach) to a dynamic one (which precise area can be exposed and how far it's possible to work within, but, *conditio sine qua non*, moving the hands properly?) (75-78). As a matter of facts, the *static* and *dynamic* anatomical dichotomy represents a fascinating debate started in the early nineties within the scientific community, due to the sudden rise of new approaches and paradigms in skull base surgery. In particular during such period, surgical anatomy was largely influenced by the concept of minimally invasive surgery: from "remove all the bone and don't touch the brain" to "don't remove the bone and don't touch the brain either through a key hole" (79-82). In such complicated debate, it was very important to understand anatomically not only "what you can see" through a new surgical window but "what you can do properly" and this was even more important when the endoscope burst on the scene of skull base surgery in late nineties. The endoscope brought the eye of the surgeon inside the surgical field but once more, the key point was: "to see and, *conditio sine qua non*, to work properly". At this point the quantitative analysis for ventral endoscopic approaches was then introduced. The quantitative analysis for endoscopic approaches brings the potential to solve problems in a systematic way by considering access to a specific anatomical region as a complex three-dimensional issue that has variables and constraints. In theory, the optimal surgical exposure is a function of target location, anatomy, and surgical pathways. The quantitative perspective creates an algorithm within the reconstructed model that solves this complex problem to optimize visualization and the ability to perform surgical tasks within the target location (83-86).

While the question of how far it was possible to see through the endonasal endoscopic route was on the way to be answered, another interrogative needed to be solved. How far it was safe to work? The experience with endoscopic transsphenoidal anatomy landed considerable insight to anatomic considerations that would limit or favor the extended endoscopic transsphenoidal approach. The purpose of anatomical investigation moved forward: from the meticulous qualitative description of the anatomical structures and their neurovascular relationship, to a quantitative and comparative analysis of the anatomical exposure between different routes (87-90).

In such way, the study of surgical anatomy slightly changed, being upgraded by modern imaging systems: anatomic knowledge needs to be integrated by complete, detailed and specific imaging platforms, in order to achieve an overall better understanding for a successful surgical procedure.

The quantification method used during the present PhD research activity was a computer-based three-dimensional anatomic model applied to the endoscopic endonasal anatomical dissections. This method enabled to obtain objective quantitative anatomical raw data (the overall surface of the removed bone) and thus enabling straight comparison between different techniques. It is based on virtual exploration and reconstruction of the anatomical route and exposure by processing pre-dissection and postdissection data in a single three-dimensional model as a result of a direct overlapped comparison of the pre- and post-dissection removed bone algorithm. The development of the computer based three-dimensional model required several tools being interfaced, above all a CT scanner (to quantify the bone), a picture archiving and communication system (PACS) and a personal computer workstation with open source digital imaging and communications in medicine (DICOM) viewer (OsiriX; Osirix Foundation, Geneva, Switzerland), a software for visualization and management of biomedical data (Amira; Visage Imaging Inc., San Diego, California, USA). A subsequent advanced quantification method was implemented by the neuronavigation system (Stealthstation®S7TM System, Medtronic) used during dissections, in order to identify critical neurovascular structures, to define the area of interest and to estimate the movement available to the surgeon's hands. This computer simulation environment naturally fits the requirements of skull base surgery, providing a detailed depiction of the surgical anatomy in a realistic three-dimensional surgical training rehearsal, with an excellent spatial perception suitable for training and for education. The application of the three-dimensional computer-based model to the endoscopic endonasal approach to the entire skull base allows analyzing, in an objective way, the main features of the surgical technique in relation to the pertinent anatomy.

Finally, the paramount importance of advanced quantitative studies was the introduction of two main parameters: the area of exposure, considered as the maximal region defined on specific deep anatomic landmarks that can be exposed using a definite surgical approach; the surgical freedom, considered as an estimate of the movement available to the surgeon's hands and instruments, represented by a partial spherical area through which surgical instruments can be inserted to manipulate a deep target. The measurements and the comparative evaluation obtained can be used preoperatively to guide the tailoring of the

surgical approach and to develop teaching surgical evidence-based guidelines. Indeed, the designed method holds the potential to play a relevant role in the design, analysis and testing of new surgical routes, as well as in the selection of the optimal approach strategy for the individual pathology of patients (84-85).

3. The application of the extended endoscopic endonasal approaches to vascular neurosurgery

The expansion of indications for the endoscopic endonasal approaches has raised the need for a detailed knowledge of the circle of Willis (CW) when exposed through this route. Familiarity with the endoscopic endonasal anatomy of the carotid and vertebro-basilar arterial systems is mandatory first of all for the safe removal of skull base lesions and nonetheless for the safe development of this approach in vascular neurosurgery (35,39,47,51,91). At the state of the art, anatomical studies focused on the feasibility of the endonasal endoscopic transsphenoidal approach to expose the CW completely are rather sparse in the literature and the application of this technique to vascular neurosurgery is still anecdotic. During tumor dissection inappropriate dealing of CW can result in injuries to a major vessels or perforators, with unacceptable mortality and morbidity. Orientation with the endonasal transsphenoidal view of circle of Willis and its branches is a fundamental step in the learning curve of skull base surgeons that usually should start from anatomical labs. Though there are sporadic reports of endonasal transsphenoidal clipping of aneurysm of CW, but most of them were done due to incidental finding of aneurysm during transsphenoidal surgery performed to address other pathologies. Scheduled aneurysm surgery is not done through this approach due to difficulty in proximal control of arteries, in retraction of surrounding brain for safe exposure of aneurysm neck for clip application, severe difficulties in dealing with intra-operative rupture of the aneurysm, less freedom in handling aneurysm clip and clip applicators, increased risk of cerebrospinal fluid leakage. To use this approach for aneurysm surgery routinely the above mentioned problem must be addressed and overcome properly. In future neurosurgeons may succeed to apply this approach for vascular neurosurgery but for that tremendous development in instruments and techniques is required (91-97).

The present manuscript resumes this PhD research activity, based on anatomical investigations integrated with clinical experience. The circle of Willis was exposed through the main extended endoscopic endonasal approaches and possible clinical applications in the

field of vascular neurosurgery were considered. The results of the research are presented in the next paragraphs following a systematic cranio-caudal anatomical order: the anterior communicating artery complex was investigated through the transtuberculum transplanum approach; the transsphenoidal approach to the sellar area was performed for the exposure of the intracavernous internal carotid artery; the basilar artery was exposed by means of the endoscopic endonasal transclival approach, and the vertebral arteries through the extended endonasal approach to the craniovertebral junction.

3.1 Endoscopic endonasal control of the paraclival internal carotid artery by Fogarty balloon catheter inflation: an anatomical study (98)

Improvements in technologies and surgical techniques have led to the expansion of more advanced endoscopic endonasal approaches, such as the fully endoscopic transnasal approach to the anterior cranial fossa, clivus, petrous bone, middle cranial fossa, and infratemporal fossa. With access to the parasellar area and the increased complexity of the addressed lesions, the danger of damaging major vascular structures raises the requirement for vascular control. One major drawback of this technique is the small surgical field and the narrow nasal corridor through which achieving vascular control and repair of main vascular injuries can be challenging. In 1993, Wascher et al. described a method of temporary petrous internal carotid artery (ICA) occlusion using a Fogarty balloon embolectomy catheter, which was placed extra-arterially within the carotid canal for cavernous sinus surgery. The aim of this anatomical study was to revisit this technique of internal carotid artery proximal control from the endoscopic endonasal route. The surgical technique, anatomical consideration, and possible clinical applications are discussed.

To perform this study, 10 fresh human cadaver heads were dissected at the Laboratory of Surgical Neuroanatomy in the Human Anatomy and Embryology Unit, Faculty of Medicine, Universitat de Barcelona, Spain. The surgical positioning of the head was simulated in the dissection laboratory; each head was slightly extended, turned 10° toward the surgeon, and fixed in a rigid 3-pin Mayfield-Kees device. Endoscopic dissections were performed using a rigid endoscope that was 4 mm in diameter and 18 cm in length with 0° and 30° optics (Karl Storz). The endoscope was connected to a light source through a fiberoptic cable and to a camera (Endovision Telecam SL, Karl Storz) fitted with 3 charge-

coupled device sensors. To obtain a suitable file of anatomical images, a digital video-recorder system was used.

Anatomical dissections were performed following the steps of the endoscopic endonasal parasseptal approach between the nasal septum and the middle turbinate. The posterior wall of the sphenoidal sinus was exposed. A bony opening was then created at the sellar floor, exposing the dura overlying the pituitary gland and thus safely gaining access to the dural layer. The bony fenestration was enlarged laterally and posteriorly as far as the paraclival ICA. A 40-cm 3-Fr Fogarty occlusion catheter (Edwards Lifesciences Corp.) was inserted at the bony opening and directed toward the paraclival carotid artery. The Fogarty catheter was then pushed downward extra-arterially (between the outer wall of the vessel and the bony wall of the carotid canal) until it naturally stopped (Fig. 1). The distal end of the catheter was connected to a 3-way stopcock that was attached to a syringe filled with normal saline solution. The balloon of the catheter was inflated with the saline solution and the stopcock was closed, providing a safe temporary occlusion of the paraclival ICA. After dissection, CT scanning (Fig. 2) and angiography (Fig. 3) were performed in each cadaveric specimen to confirm the positioning of the Fogarty balloon catheter and ICA occlusion. We found a volume of 5 ml of saline solution to be optimal for achieving interruption of blood flow across the paraclival ICA. The described technique was performed during 2 surgical cases of pituitary macroadenoma with cavernous sinus invasion (Fig. 4A–D).

Neurosurgical management of many vascular and neoplastic lesions necessitates control of the ICA, e.g., aneurysms of the paraclinoidal region, tumors invading the cavernous sinus, and skull base tumors. Traditionally, exposing the cervical carotid vessels and placing temporary clips on the cervical ICA can obtain proximal control of the internal ICA. However, neck dissection requires a separate incision and presents the distinct disadvantage of 2 separate operative fields should immediate control of bleeding be necessary, in addition to esthetic considerations. When proximal control of the arterial blood supply to the cavernous sinus region is needed, these disadvantages might be overcome by means of occlusion of the petrous ICA with aneurysm clips or packing material within the carotid canal. Safe exposure of the petrous ICA requires thorough knowledge of the anatomical landmarks of the floor of the middle cranial fossa and is not without the potential for serious complications, such as hearing loss, facial palsy from traction injury to the greater superficial petrosal nerve, or laceration of the ICA when unroofing the carotid canal. After the initial exposure, the ICA must be separated from its sheath of periosteum, venous channels, and sympathetic nerve fibers in order to allow placement of temporary aneurysm

clips in preparation for grafting or temporary occlusion of the petrous ICA segment. This extradural approach has been modified by performing a transdural exposure of the petrous ICA and occluding the ICA temporarily with a Fogarty balloon catheter that is placed extra-arterially within the proximal carotid canal. This modification is faster and technically simpler than the complete circumferential dissection of the petrous ICA that is required when the occlusion is to be provided by the application of temporary aneurysm clips. Endovascular balloon inflation has also been used to achieve both proximal and distal control of the ICA during aneurysm surgery and proven to be extremely helpful in interrupting local blood flow. The advantages of this technique include greater exposure of the aneurysm for permanent clipping due to the elimination of the need for temporary clips, the improved accuracy of clip placement, and the reduction of the risk of intramural aneurysm thrombus dislodgment due to multiple temporary clipping. However, there are several disadvantages to the routine use of endovascular intraoperative techniques. A dedicated interventional radiologist must stay in the operating room during surgery. Some degree of radiation exposure for the patient and the operating room personnel is unavoidable during an intraoperative angiography procedure. The additional time required for the endovascular setup and intraoperative angiography is usually around 1 hour. The addition of endovascular adjuncts to aneurysm surgery may be associated with potential embolic complications.

In this anatomical study, we investigated the feasibility of achieving control of the ICA through the endoscopic endonasal approach by temporary occlusion with a Fogarty balloon catheter. In our opinion, using a Fogarty catheter rather than temporary aneurysm clips is well suited to endoscopic endonasal surgery. The complete circumferential dissection of the ICA that is required when the occlusion is to be provided by the application of temporary aneurysm clips may be complicated by the small and deep corridor provided by the endonasal route. Furthermore, the use of a Fogarty catheter instead of vascular clips increases the available space to perform surgical maneuvers around the ICA. In this anatomical study, temporary occlusion of the ICA with a Fogarty balloon catheter was achieved in all cases through a parasseptal approach, which can be considered a fast, safe, and minimally invasive procedure. Exposure of the ICA bilaterally in the sellar region can be achieved with this approach with no need for the removal of the middle turbinate. The paraclival segment of the ICA is easily recognized and accessed. Occlusion of the ICA is gained extradurally, thus eliminating the risk of cerebrospinal fluid leakage, which is often associated with the majority of endoscopic endonasal procedures. If the interruption of blood flow across the ICA has to be obtained by compression, the Fogarty balloon catheter has to

be inflated where the vessels are surrounded by rigid structures. Otherwise, the ICA will be displaced and not occluded, with the risk of damaging other anatomical structures. Theoretically, the petrous ICA at the foramen lacerum fulfills this anatomical and functional criterion. We started anatomical dissections with the aim of inflating the Fogarty catheter at this level, thus compressing the artery against the bone of the posterior wall of the sphenoidal sinus ventrally, the petroclival junction medially, the dura of the temporal lobe laterally, and the fibrous lower portion of the foramen lacerum dorsally. During our study, however, we found that the catheter naturally stops before reaching the petrous ICA along the course of the paraclival ICA, where it hits the inferior petrosal ligament or any other bony prominence. The encasement of the paraclival ICA was rigid enough, thus allowing for it to be compressed and occluded by the Fogarty balloon without needing to reach the foramen lacerum. The important neurovascular structures at this level are the posterior apex of the cavernous sinus and the sympathetic fibers traveling from the surface of the carotid to the abducens nerve before ultimately being distributed to the first trigeminal division. Since compression is temporal and causes minimal displacement of the ICA, this anatomical relationship should not represent a contraindication to the technique. Temporary occlusion with a Fogarty catheter balloon of the paraclival ICA through the endoscopic endonasal paraseptal approach can be used, should intraoperative rupture of the vessel occur. Operating around the ICA creates the possibility of its rupture. The endoscopic endonasal approach is minimally invasive and access to the ICA is minimal. This is especially true in the case of endoscopic endonasal skull base surgery due to the long narrow surgical corridor and the difficulty of maintaining endoscopic vision of the injury within a visual field that becomes quickly obscured. Internal carotid artery injury during endoscopic pituitary surgery is an infrequent event, with an incidence of 0.5% to 1.1%. However, more extended endoscopic resections have a higher incidence of ICA rupture at 4% to 9%. We reported 2 surgical cases of pituitary macroadenoma invading the cavernous sinus that we considered at high risk for ICA injury. The Fogarty balloon catheter was positioned at the paraclival ICA before tumor removal was started. In the case of rupture of the artery, this would have given us the chance to temporally control the surgical field, avoiding indiscriminate nasal packing and vascular occlusion and perhaps reducing complications and saving the patient's life. Once the surgical field is controlled, hemostatic techniques can be implemented under endoscopic visualization or, if necessary, by resorting to other surgical or endovascular maneuvers. The technique of ICA temporary occlusion may be a useful option during the removal of highly vascularized tumors of the suprasellar region, cavernous sinus, and anterior cranial fossa. By occluding the

artery, blood flow to the tumor can be reduced, thus facilitating its debulking. The application of endonasal surgery remains controversial for vascular lesions. The technique we described in this study could simplify achieving proximal control of the ICA in the setting of endoscopic endonasal surgery for a vascular lesion in the anterior circulation. Given the limited visualization area, circumferential dissection of the ICA to allow placement of temporary clips may be complicated, especially in the setting of intraoperative rupture. Positioning temporary clips further reduces the surgical space, complicating dissection of the aneurysm and clipping of the neck with preservation of the perforators. Control of the proximal anterior communicating arteries, which are hidden above the optic nerves and chiasm, can be risky. A potential bilateral occlusion of the paraclival ICA by compression with a Fogarty balloon may allow for the control of contralateral blood flow across an anterior communicating artery aneurysm. Besides the application of the temporary occlusion of the paraclival ICA with a Fogarty balloon catheter to pure skull base endoscopic endonasal surgery, this technique might be considered for cases that use endoscope-assisted transcranial microsurgical approaches. When vascular control of the ICA has to be planned before starting transcranial surgery, e.g., for paraclinoidal aneurysm surgery, an endoscopic endonasal parasseptal approach can be performed and the Fogarty catheter left in situ as an alternative to exposing the cervical carotid vessels or performing endovascular techniques. The balloon may then be inflated or not, depending on the surgical needs. In our experience, Fogarty balloon placement into the paraclival ICA canal results in a fast and easy procedure. The average time for balloon positioning could be estimated to be between 3 and 10 minutes. A 4-hand technique is required, with 1 surgeon holding the endoscope and the instrument, and the other inserting the catheter from the contralateral nostril and keeping the surgical field clean with aspiration. Once the Fogarty catheter appears in the sphenoid cavity, it must be directed antero-posteriorly, with its distal end leaning on the planum sphenoidale. The catheter is brought closer to the paraclival ICA and pushed extra-arterially along the artery with the use of grasping forceps, taking care not to damage the balloon by grasping the catheter too close to its proximal end. Bone removal at the sellar floor is minimal, just as much as is required to access the dural plane. Exposing the dura of the sella and then extending the bone removal laterally toward the paraclival ICA is probably safer than a straight exposure of the artery by drilling the paraclival bone protuberance. Exposure of the paraclival ICA is reduced to its identification, with no need for wider visualization of the artery. The Fogarty balloon is inserted extra-arterially along the paraclival ICA with a direction parallel to the course of the artery. No specific angulation of the catheter is required

since it will naturally advance along the ICA, as any other direction is obstructed by the rigid bony and dural structures that encase the carotid at this level. Once the surgeon feels any resistance when inserting the Fogarty catheter extra-arterially along the paraclival ICA, the maneuver should stop. Any attempt to further push the Fogarty catheter could cause rupture of the balloon against bony edges. Insertion of the balloon for a few millimeters inside the paraclival ICA canal is enough to obtain the vessel's compression and occlusion when the balloon is inflated (Fig. 5). The potential risks and complications of temporary occlusion of the paraclival ICA are stroke and thrombo-embolism. Neuromonitoring of brain activity, e.g., with electroencephalography or evoked potentials, is recommended during surgery. Another possible complication could be direct damage to the carotid artery by positioning and inflating the Fogarty balloon. In our study, we did not experience this. Postoperative CT or MR angiography could allow for the assessment of ICA patency at the same time as the extension of lesion removal. The presence of the Fogarty catheter inside the small surgical area provided by the endoscopic endonasal approach to the cavernous sinus region could represent an impediment during tumor removal. However, in our experience, we were able to remove the cavernous portion of the pituitary adenomas. Because of its small diameter, the Fogarty catheter does not obstruct the entrance of any other surgical instruments. It is flexible and it can be sutured outside the nasal cavity; thus, the Fogarty balloon would not accidentally exit the paraclival ICA canal during surgical maneuvers.

This anatomical study shows that temporary occlusion of the paraclival ICA with a Fogarty balloon catheter through the endoscopic endonasal route might be another maneuver that is useful for obtaining intraoperative control of the vessel, which is an alternative to complex microsurgical approaches that expose the petrous ICA, temporary clips in the surgical field, or endovascular techniques. It is a fast, safe, minimally invasive, and potentially temporary bilateral technique. This study also demonstrates another means by which the endonasal endoscopic approach can enhance the neurosurgical armamentarium. Further clinical studies are needed to prove the efficacy of this method.

3.2 Endoscopic endonasal surgery for a mesencephalic cavernoma (99)

The report of the following case of a ventral midline mesencephalon cavernous malformation approached through the endoscopic endonasal route (Fig.6) deserves

consideration in that the localization of the cavernous malformation, the clinical presentation consisting of an isolated third-nerve palsy without other non-ocular signs and the surgical approach used are rather unusual. Surgery was performed at the Department of Neurosurgery, Hospital Clinic, University of Barcelona, Spain.

Possible approaches to access cavernomas in this location include: a subfrontal route, superior to the anterior cerebral artery, Heubner's artery and optic tract, or through the lamina terminalis; an approach through the ventricle (transcallosal, subchoroidal, transventricular approach); or between perforators coming off the M1 segment of the middle cerebral artery. However, these approaches offer a limited exposure of the ventral midbrain, through a narrow corridor between the cranial nerves and vascular vital structures, besides requiring a certain amount of brain manipulation. Bricolo et al. described a safe entry zone into the anterior midbrain, which allows surgical access through the more medial part of the peduncle, sparing the motor tract. In the present case, entering the midbrain through this safe entry zone would still be a relatively indirect route to this cavernoma located medially to the third nerves, bringing the problem of traversing the third nerve or the necessity of its transposition. It was decided that, because of the location of the cavernoma surfacing at the midline ventral midbrain, the endoscopic transnasal transtuberculum transplanum approach could offer the straightest and safest route to the lesion. Surgeon comfort was also considered in favor of the endoscopic endonasal skull base technique.

Major issues in favor of surgery were: the pial presentation of the cavernoma surfacing at the ventral mesencephalon, thus allowing for a purely trans-lesional resection through a direct anterior approach and avoiding the need of transverse intact neural tissue; and the neurological status of the patient, which remained substantially stable during the 3 weeks after the acute onset and that the patient considered incompatible with his daily life.

At surgery, once the interpeduncular fossa was entered, moving the endoscope further in the surgical field allowed for the clear visualization of the basilar artery in the center of the surgical field, the mammillary bodies superiorly, the cerebral peduncles and the posterior communicating arteries laterally, and the oculomotor nerves and the posterior cerebral arteries inferiorly. The hematoma overlying the cavernous malformation was encountered on the ventral surface of the midbrain. Removing a small portion of normal pituitary gland increased the working area. Pituitary gland transposition and posterior clinoidectomy could have been possible adjunct techniques that were considered when surgery was started, if the surgical corridor was too narrow. However, a standard transplanum transtuberculum approach allowed for a comfortable exposure of the cavernoma and the surrounding

neurovascular structures. The pathology itself was creating the space between the mesencephalon and the basilar artery, the posterior communicating arteries and the perforators. With the assistance of gentle suction and sharp dissection, the hematoma was evacuated and the cavernoma removed in a piecemeal fashion, decompressing the brainstem. Evacuating the hematoma together with fragments of the cavernoma eliminated this virtual space. Then, the anatomical orientation made it too risky to attempt any other surgical maneuver and the surgery was stopped without having the chance of deeply inspecting the surgical cavity, which resulted in a subtotal removal of the cavernoma. The encountered situation could not probably be overcome with any other approach, but with an en bloc removal. Postoperatively, the patient's oculomotor symptoms were entirely solved and no new neurological or endocrinological deficit appeared.

The unique features of this particular case may provide valuable information to surgeons choosing to tackle such difficult lesions.

3.3 Quantitative anatomical analysis of the endoscopic assisted lateral supraorbital approach and endoscopic endonasal transclival approach: two minimally invasive routes to basilar apex aneurysms.

Basilar apex aneurysms are among the most challenging to treat with microsurgical clipping. Due to their deep location and intimate relationship with the brainstem, cranial nerves, and perforating branches, they are associated with a high morbidity rate. Furthermore, since the endovascular techniques have become a viable alternative of treatment, there has been a heightened demand for improved patient outcomes after surgery (100-113). For these reasons, the investigation of alternative microsurgical techniques in treating basilar apex aneurysms is warranted. Classically, the pterional and subtemporal approaches have been used to clip aneurysms of the upper basilar trunk, the choice being based first of all on the relative anatomical conformation of the basilar apex and dorsum sellae (114). The subtemporal approach described by Drake (115) and further developed in recent decades is the most frequently used approach for operating on basilar tip (116-119). Retraction of the temporal lobe is necessary and should be done carefully to minimize the risks of temporal lobe contusions or injury to the vein of Labbè. For sufficient exposure of the basilar artery below the basilar quadrifurcation, an incision of the edge of the tentorium may be necessary (120). The second most frequent approach for upper posterior circulation aneurysms,

according to the literature, is the frontotemporal approach (121-126). After performing a frontotemporal craniotomy, it is necessary to dissect the Sylvian fissure widely to obtain enough space for the aneurysm dissection via carotid-oculomotor corridor. It is often necessary to open the cavernous sinus and to remove the posterior clinoid process (127-134). Many variants have been proposed to the pterional and sub-temporal approaches in order to reduce their limits, but increasing the complexity of the approach corresponds to a greater risk of vascular and neural structures damage (135-136). In the trend of minimize extended skull base approaches, more attention has been dedicated lately in the literature to the lateral supraorbital approach (LSO) and the endoscopic endonasal transclival approach (EETA) (137-148). Each basilar trunk aneurysm requires an individualized surgical strategy that takes into account its angioarchitecture, its relationship with surrounding bony and neural structures, surgeon experience and patient's condition. Improvement in diagnostic imaging pre-operative planning tools allows for the choice of the safest and less invasive approach tailored to each patient. In very selected cases the LSO and EETA may represent a valid surgical option. The aim of this study is to quantitatively evaluate the lateral supraorbital approach and the endoscopic endonasal transclival approach with respect to anatomical exposure and surgical freedom around the basilar apex. Endoscopy was further evaluated with regard to its usefulness in assistance in the lateral supraorbital approach. Quantitative anatomical information may allow a pre-operative assessment of the validity of these surgical routes to the basilar apex and eases the decision as to which approach best suits each patient.

Twenty formaline-fixed cadaveric heads were used for anatomical dissections. Cerebral arteries were injected with a colored silicone rubber mix through carotid and vertebral arteries. Dissections were performed at the Laboratory of Surgical NeuroAnatomy in the Human Anatomy and Embryology Unit, Faculty of Medicine (Universitat de Barcelona, Barcelona, Spain).

For each specimen, before dissection, radiological images were obtained in a multislice helical computed tomography (CT) scanner Siemens® SOMATOM Sensation 64 with axial spiral sections of 0.6 mm thick without X-ray tube inclination factor. Cadaveric heads were positioned to simulate the surgical position in the operating room in a rigid three-pin Mayfield-Kees device to allow the use of the neuronavigation systems (Stealthstation®S7TM System, Medtronic). Neuronavigation data were processed by specific software for visualization and manipulation of biomedical data (Amira® Visage Imaging Inc., San Diego) in order to quantify anatomical exposure and surgical freedom around the anatomical area of interest. During microsurgical dissection, an operative microscope

(OPMI; Zeiss, Oberkochen, Germany) was used with possible magnification ranging from 4X to 40X. Digital images were obtained during dissections. During endoscopic dissection, we used a 4-mm-diameter endoscope, measuring 18 cm in length, with 0-degree rod-lenses (Karl Storz GmbH and Co., Tuttlingen, Germany). The endoscope was connected to a light source through a fiberoptic cable and to a camera (Endovision Telecam SL; Karl Storz) fitted with three charge-coupled device sensors. Both video and digital images were obtained during dissection.

On ten cadaveric heads a right lateral supraorbital approach was performed as previously described by Hernesniemi et al. The head was rotated 15 degree toward the left side and a short oblique frontotemporal incision was performed. A small frontal craniotomy exposing the superior orbital rim and the anterior zygomatic arch was performed. The lateral sphenoid wing was drilled off; the dura mater was opened and the Sylvian fissure was splitted from the frontal side. The basilar apex was reached through a corridor between the right optic nerve and the right internal carotid artery (ICA) by microsurgical dissection in a medio-lateral direction, until the posterior communicating artery (PcomA) was identified. The PcomA was followed along the inferior surface of the temporal lobe to its origin from the posterior cerebral artery. The supraclinoid tract of the ICA was medially withdrawn together with PcomA, to increase visibility through the oculomotor-carotid corridor (Fig.7A). The spatula remained rigidly fixed with sufficient strength so as not to damage the supraclinoid ICA and its perforating arteries. The oculomotor nerve was identified laterally to the ICA and deeply to posterior cerebral artery in its distal course (P2). The third cranial nerve runs inferiorly to the tentorial margin where it reaches the posterior clinoid process. Opening of the arachnoid membrane between the posterior clinoid process and the third cranial nerve allows for exposure of the Liliequist membrane and basilar apex in the interpeduncular cistern (Fig.7B). Lateral to the oculomotor nerve, the superior cerebellar artery running on the tentorial edge with the fourth cranial nerve can be seen (Fig.8). The lateral supraorbital approach was completed with right posterior clinoidectomy. Finally, the endoscope was introduced into the surgical field (fig.9).

On ten cadaveric heads an endoscopic endonasal transclival approach was performed, following the surgical steps that have been already extensively described. Bone removal was extended from the floor of the sella inferiorly to 2/3 of the clivus (fig.10A). The dura was opened on the midline and prepontine cistern and vessels inside it were exposed free from arachnoid (fig.10B). The approach was completed with drilling of the dorsum sellae.

The average extent of exposure of the upper basilar artery complex, i.e. posterior

cerebral artery (PCA), superior cerebellar artery (SCA) and basilar artery, was measured as provided by the two approaches. With regard to LSO, measurements were taken before and after posterior clinoidectomy was performed and after the introduction of the endoscope in the operative field. With regard to EEA, measurements were taken before and after drilling of the dorsum sellae. Relevant anatomical structures limiting the maneuverability of surgical instruments around the basilar apex were identified as targets for the calculation of the average area of surgical freedom.

Once the interpeduncular cistern was reached through the LSO, the basilar apex was visualized in all specimens. Limits of anatomical exposure corresponded to: the posterior clinoid process anteromedially, the anterolateral surface of the midbrain postero-medially, and the III cranial nerve laterally running along the temporal surface of the cranial base. Surgical freedom, calculated as $33,2 \text{ mm}^2 (\pm 6,8 \text{ mm}^2)$, was limited by these structures. The posterior clinoid process occluded anatomical exposure to the basilar artery tip and ipsilateral posterior cerebral artery for an average length of $11,4 \text{ mm} (\pm 2,6 \text{ mm})$. In our study, we didn't find any upper basilar artery complex higher than dorsum sellae and posterior clinoid. Indeed, posterior clinoidectomy was performed in all specimens.

Right posterior clinoidectomy increased surgical freedom up to $54,3 \text{ mm}^2 (\pm 7,5 \text{ mm}^2)$, which was now calculated using the root of the posterior clinoid process as anteromedial limit. Anatomical exposure expanded inferiorly and controlaterally: basilar trunk became visible for $4,6 \text{ mm} (\pm 2,8 \text{ mm})$ caudally from its apex, controlateral PCA was exposed for $6,2 \text{ mm} (\pm 4,3 \text{ mm})$, while ipsilateral exposure remained unchanged (fig.11A-B).

Endoscopic assistance in the LSO allowed for a wider exposure caudally: the basilar trunk became visible for $7,4 \text{ mm} (\pm 3,7 \text{ mm})$, superior cerebellar artery (SCA) was exposed for $9,6 \text{ mm} (\pm 5,2 \text{ mm})$ ipsilaterally and for $3,9 \text{ mm} (\pm 2,8 \text{ mm})$ controlaterally. Only with an endoscope-assisted approach both SCA could be visualized and the exposure became similar to that reached with an EETA. Even though endoscopic assistance increased the anatomical exposure provided by the LSO, surgical freedom didn't change due to its fixed limits given by anatomical structures that cannot be overcome.

The EETA allowed for exposure of the basilar apex and SCA bilaterally in every specimen. Limits of anatomical exposure corresponded to the edges of dural opening. By drilling the 2/3 of clival bone, the basilar trunk was exposed for an average of $8,7 \text{ mm} (\pm 4,6 \text{ mm})$ and SCAs for $5,8 \text{ mm} (\pm 3,6 \text{ mm})$ as average between right and left side. Indeed, the EETA offers the best bilateral caudal exposure around the basilar apex, with a surgical freedom corresponding to $46,2 \text{ mm}^2 (\pm 12,6 \text{ mm}^2)$. The exposure and control of posterior

cerebral arteries was limited by dorsum sellae, with minimum exposure of PCAs of 3,1 mm ($\pm 3,2$ mm) on average between right and left side. In order to increase the area of maneuverability and control of PCA, it was necessary to drill the dorsum sellae: thus surgical freedom resulted 101,3 mm² ($\pm 23,6$ mm²) and PCAs exposure of 5 mm ($\pm 2,7$ mm) on average bilaterally. Exposure of basilar trunk increased for 3,4 mm ($\pm 4,1$ mm) cranially (fig.12).

Quantification of anatomic laboratory investigation allowed us to draw the following results. The relationship between basilar apex and dorsum sellae together with posterior clinoids process should guide the choice of best surgical approach in and around the basilar artery. The LSO provides an insufficient anatomical exposure and surgical freedom in and around the upper basilar artery complex, being visualized only the basilar apex and ipsilateral PCA for a short length, unless an high-lying basilar artery is found. Expansion of the LSO with posterior clinoidectomy increases both measurements. It offered a wider surgical freedom around the basilar apex together with visualization and control of the basilar trunk, ipsilateral and contralateral PCA. The increased exposure of the top of the basilar artery and its branches with a posterior clinoidectomy means that this approach is of value for visualization and control of the upper basilar artery complex when it is not lower than 4,6 mm from the dorsum sellae. Endoscopic assistance was found to be an effective way to image both the ipsilateral and contralateral aspects of the area around the basilar apex, downward to the SCAs. In this way, a safe visualization of the basilar artery and its parent vessels could be achieved. The EETA expanded with drilling of dorsum sellae offers the widest area of surgical freedom around the basilar apex, with visualization of the whole basilar artery complex. However, exposure and control of PCAs remained limited. The increased exposure of the basilar artery with drilling of dorsum sellae means that this approach is of value for visualization and control of the vessel and its branches when the basilar apex is not higher than 3,4 mm from the dorsum sellae. Drilling of both posterior clinoid processes and pituitary transposition could increase anatomical exposure and surgical freedom with the disadvantage of the invasiveness related to such maneuvers.

Hernesniemi proposed the LSO (137) as an alternative to the standard pterional approach (121,126). The impetus for this approach, referred to as minimally invasive approach, has been its minimal interference with the temporalis muscle, sphenoid wing, cosmetic considerations such as hiding the skin incision in the eyebrow, reduced exposure and dissection of the sylvian fissure, less risk of oculomotor nerve palsy and of temporal lobe injury due to retraction. However, a sound neurosurgical approach needs to achieve a careful

balance between minimizing tissue trauma and maximizing anatomic exposure and safe operability. Careful understanding of this modified surgical route, of the anatomic areas to which it offers access, and of the operability associated with it is important for recognizing the limitations and advantages of the approach. The LSO provides a limited angle of view of the interpeduncular cistern region owing to a subfrontal trajectory. Posterior clinoidectomy has been already advocated as a maneuver to overcome this limit, always when basilar apex is at the level of below the dorsum sellae. In the present study we quantified the increased anatomical exposure and surgical freedom associated with removal of posterior clinoid process, identifying 4,6 mm as the lowest position of the upper basilar complex from the dorsum sellae to safely address BA aneurysms through a LSO. For the first time, we have also investigated a promising alternative that may aid in this respect: the use of the endoscope to expand anatomical exposure provided by the LSO after posterior clinoidectomy. Endoscopic assistance allows for exposure of the whole basilar artery complex without extra surgical exercise, with visualization of posterior cerebral arteries, superior cerebellar arteries and basilar trunk. However, based on our results, endoscopic assistance still may not fully address the challenges of maneuvering instrumentation in the limited space. We recommend that it be used to aid in inspection of the basilar perforators and contralateral vessels arising from the basilar artery. This can be done with minimal morbidity, imparting an added measure of safety and efficacy in enabling the assessment of clip placement and the patency of surrounding vessels.

Recently, the endoscopic endonasal technique has been advocated as a suitable option to complement the role of traditional microsurgical and endovascular techniques in the care of patients with very selected vascular intracranial pathologies, such as paraclinoid and ventral posterior fossa aneurysms that may be challenging due to their inherent characteristics such as location, accessibility, shape, and configuration (145-148). The main components of the vertebrobasilar system may be easily exposed through an (EETA). In fact, this approach is the only one to provide a direct route to these vessels without more extensive open exposure and some degree of brain retraction. For this reason, the EETA has often been referred as minimally invasive. In our study, we quantified the anatomical exposure and surgical freedom in and around the interpeduncular cistern when reached by an endoscopic endonasal transclival route extended by drilling of dorsum sellae. We identified the safely cut-off of upper basilar complex distance from the dorsum sellae as 3,4 mm. A higher basilar apex excludes the feasibility of this approach, remaining the basilar apex and PCAs out of the view. Extradural or interdural pituitary transposition posterior clinoidectomy would then be

required and the option of a less complex approach should be considered.

Modern diagnostic imaging offers the advantage of defining accurately anatomic and pathologic structures and the topographic relationship of these structures down to dimensions of about 1 mm. These precise diagnostic imaging techniques enable the surgeon to carry out preoperative surgical planning with the same amount of precision. Surgical treatment of BA aneurysms requires an individualized strategy that takes into account the aneurysm configuration, the angioarchitecture, and the patient's condition. Based on quantitative information acquired in the anatomical lab and pre-operative imaging studies, the surgeon is called to tailor the approach on specific feature of the pathology and surrounding anatomical configuration. Only when this is accomplished a surgical approach should be defined minimally invasive, independently from the dimension of skin incision, bone removal or navigation around vital neurovascular structures. Our study may add relevant quantitative information to the present literature in the knowledge of limits and advantages of the LSO and EETA, aiding in determining the correct indications for each procedure. Using the advantageous features of these approaches will help to deliver the treatment that is the most appropriate for each individual patient, allowing for the decision as to which approach results minimally invasive for each patient.

The choice of the operative approach generally depends on the size, shape, exact localization and direction of aneurysm projection of the intracranial aneurysm, the degree of brain swelling, other patient comorbidities, and surgeon's experience. Relevant preoperative radiological characteristics include basilar bifurcation angle, PCA symmetry, presence of a fetal posterior cerebral artery, and vertical distance from aneurysm neck to dorsum sellae and posterior clinoid process. A major limit of the present study was the impossibility of reproducing so many variables in an anatomical lab environment. Still, we focused our quantitative evaluation of the endoscopic assisted LSO and EETA on the relationship of upper basilar complex with dorsum sellae, a main factor determining surgical approach. We provided relevant information to demonstrate the anatomic capacity of these approaches to the basilar apex, highlighting and quantifying the possibility of safely performing appropriate surgical maneuvers. Clearly, the ability to carry on this information from a cadaver environment to a live surgery environment needs to be validated clinically. By adding relevant quantitative anatomical information, our study may be helpful in determine the best indication for the endoscopic assisted LSO and EETA in the treatment of basilar apex aneurisms. Surgeons who perform basilar aneurysm surgery should be aware of these techniques and their occasional minimal invasive role, intended as the safest surgical

approach in the presence of specific anatomical and pathological conditions.

3.4 Comparative exposure of the vertebral artery at the cranio-vertebral junction through transcranial and extended endoscopic endonasal approaches.

Cranio-vertebral junction (CVJ) refers to the complex transition from the skull to the spine. Its bony structure consists of the occipital bone, atlas (C1), and axis (C2). Muscles, ligaments and membranes that provide stability and mobility to the craniovertebral junction support the bony structure of this critical region. Major neurovascular structures are intimately related to the CVJ where they transverse membranous and bony orifices. These include the lower cranial and upper spinal nerves, the caudal brainstem and rostral spinal cord, the vertebral artery and its branches, and the venous drainages through the jugular vein and the vertebral plexus.

The transcranial far lateral and the endoscopic endonasal approaches to the antero-lateral aspect of the brainstem at the craniovertebral junction allow for access to this complex area of the skull base, both providing exposure and control of the vertebral artery, by two different, complementary, routes (88, 153-156).

A thorough understanding of three-dimensional (3D) CVJ anatomy and relations with the vertebral artery and surrounding neural structures is paramount for surgical management of pathologies in this region. Merging together anatomical information coming from endoscopic and microsurgical investigations with the reconstruction of 3D computed models might provide a 360° full and clear understanding of this complex area, more readily applicable to the operative setting.

The postero-lateral perspective of the CVJ is directed at the condylar part of the occipital bone, and lateral masses of atlas and axis (fig.13). Through this perspective, the segment of the vertebral artery extending from the transverse foramen of C2 to its entrance to the dura is exposed (V3). The artery, after ascending through the transverse process of the atlas, is located on the medial side of the rectus capitis lateralis muscle. From here it turns medially behind the lateral mass of the atlas and the atlanto-occipital joint and is pressed into the groove on the upper surface of the posterior arch of the atlas, where it courses in the floor of the sub-occipital triangle (fig.14). The triangle is not always easy to identify because of the thick fascia, which covers the deepest layer of the posterior neck muscles. This fascia and the underlying fat and the rich paravertebral venous plexus obscure the anatomical relationship

of these muscles (fig.15). The intradural segment of the vertebral artery (V4) can be divided in a lateral medullary segment and an anterior medullary segment. The V4 lateral medullary segment begins at the dural foramen and passes anterior and superior along the lateral medullary surface to terminate at the pre-olivary sulcus. The posterior inferior cerebellar artery (PICA) enters this cistern after originating from the fourth segment (V4) of the vertebral artery intra-durally. In the cerebello-medullary cistern the PICA passes dorsally between the rootlets of the IX, X and XI cranial nerve and pursues a posterior course around the medulla (fig.16).

The antero-medial perspective of the CVJ provides exposure of the clival portion of occipital bone, anterior border of foramen magnum, anterior arch of C1, and the odontoid process (fig.17). Intradurally, the anterior medullary segment of the vertebral artery (V4) is exposed. It begins at the pre-olivary sulcus, courses in front of, or between, the hypoglossal rootlets, and crosses the pyramid to join with the other vertebral artery at or near the ponto-medullary sulcus to form the basilar artery (fig.18).

Multiple cranial base approaches have been described to manage lesions located in the lower third of the clivus and the cranio-cervical junction. The lower cranial nerves and the posterior arterial circulation, mainly the vertebral artery, divide the posterior fossa into ventro-medial and dorso-lateral compartments. Most trans-cranial approaches to the posterior fossa are limited ventro-medially by these structures. The extended endoscopic approach to the CVJ, although proven to be effective and safe for treating median pathology, is limited in accessing lesions located in the dorso-lateral compartment. Therefore, an accurate knowledge of the neurovascular structures that divide the posterior fossa is paramount in selecting the best option for accessing each lesion. A ventral endoscopic endonasal approach offers a safe and wide exposure of the lower third of the clivus. It is particularly superior for lesions that expand ventro-medially from the vertebral artery. The microsurgical far lateral approach is the traditional and most appropriate approach for the lesions located dorsolateral to the vertebral artery. A combined endoscopic endonasal approach/ far lateral approach is a strategy that could be indicated in selected cases of complex lesions affecting ventro-medial compartment and dorso-lateral compartment simultaneously (153-156).

References

1. Carrau RL, Jho HD, Ko Y. Transnasal-transsphenoidal endoscopic surgery of the pituitary gland. *Laryngoscope*. 1996;106(7):914-918.
2. Jho HD, Carrau RL. Endoscopy assisted transsphenoidal surgery for pituitary adenoma. Technical note. *Acta Neurochir (Wien)*. 1996;138(12):1416-1425.
3. Jho HD. Endoscopic transsphenoidal surgery. *J Neurooncol*. 2001;54(2):187-195.
4. Hardy J. Trans-sphenoidal approach to the pituitary gland. In: W i i RH, Flengachary SS, eds. *Neurosurgery*. New York: McGraw-Hill Book Co., 1983:889-898.
5. Rosegay H. Cushing's legacy to transsphenoidal surgery. *J Neurosurg*. 1981;54:448-454.
6. Griffith HB, Veerapen R. A direct transnasal approach to the sphenoid sinus. Technical note. *J Neurosurg*. 1987;66:140-142.
7. Wilson WR, Khan A, Laws ER Jr. Transseptal approaches for pituitary surgery. *Laryngoscope*. 1990;100:427-442.
8. Cooke RS, Jones RAC. Experience with the direct transnasal transsphenoidal approach to the pituitary fossa. *Br J Neurosurg*. 1984;8:193-196.
9. Cappabianca P, Alfieri A, Colao A, Ferone D, Lombardi G, de Divitiis E. Endoscopic endonasal transsphenoidal approach: an additional reason in support of surgery in the management of pituitary lesions. *Skull Base Surg*. 1999;9(2):109-117.
10. Cappabianca P, Alfieri A, de Divitiis E. Endoscopic endonasal transsphenoidal approach to the sella: towards functional endoscopic pituitary surgery (FEPS). *Minim Invasive Neurosurg*. 1998;41(2):66-73.
11. Cappabianca P, de Divitiis E. Endoscopy and transsphenoidal surgery. *Neurosurgery*. 2004;54(5):1043-1048.
12. Wang AJ, Zaidi HA, Laws ED Jr. History of endonasal skull base surgery. *J Neurosurg Sci*. 2016 Dec;60(4):441-53.
13. de Divitiis E, Laws ER, Giani U, Iuliano SL, de Divitiis O, Apuzzo ML. The current status of endoscopy in transsphenoidal surgery: an international survey. *World Neurosurg*. 2015 Apr;83(4):447-54.

14. Doglietto F, Prevedello DM, Jane JA Jr, Han J, Laws ER Jr. Brief history of endoscopic transsphenoidal surgery--from Philipp Bozzini to the First World Congress of Endoscopic Skull Base Surgery. *Neurosurg Focus*. 2005 Dec 15;19(6):E3.
15. Zada G, Liu C, Apuzzo ML. "Through the looking glass": optical physics, issues, and the evolution of neuroendoscopy. *World Neurosurg*. 2013;79(2 Suppl):S3-13.
16. Aryan HE, Hoeg HD, Marshall LF, Levy ML. Multidirectional projectional rigid neuro-endoscopy: prototype and initial experience. *Minim Invasive Neurosurg*. 2005;48(5):293-296.
17. Levy ML, Nguyen A, Aryan H, Jandial R, Meltzer HS, Apuzzo ML. Robotic virtual endoscopy: development of a multidirectional rigid endoscope. *Neurosurgery*. 2008;62 Suppl 2:599-606.
18. Oi S, Samii A, Samii M. Frameless free-hand maneuvering of a small-diameter rigid-rod neuroendoscope with a working channel used during high-resolution imaging. Technical note. *J Neurosurg*. 2005;102(1 Suppl):113-118.
19. Cavallo LM, Di Somma A, Solari D, de Divitiis O, Bracale UM, Cappabianca P. Preliminary experience with a new multidirectional videoendoscope for neuroendoscopic surgical procedures. *PLoS One*. 2016;11(1):e0147524.
20. Felisati G, Lenzi R, Pipolo C, Maccari A, Messina F, Revay M, Lania A, Cardia A, Lasio G. Endoscopic expanded endonasal approach: preliminary experience with the new 3D endoscope. *Acta Otorhinolaryngol Ital*. 2013 Apr;33(2):102-106.
21. Ogino-Nishimura E, Nakagawa T, Sakamoto T, Ito J. Efficacy of three-dimensional endoscopy in endonasal surgery. *Auris Nasus Larynx*. 2015;42(3):203-207.
22. Felisati G, Pipolo C, Maccari A, Cardia A, Revay M, Lasio GB. Transnasal 3D endoscopic skull base surgery: questionnaire-based analysis of the learning curve in 52 procedures. *Eur Arch Otorhinolaryngol*. 2013;270(8):2249-2253.
23. Shah RN, Leight WD, Patel MR, Surowitz JB, Wong YT, Wheless SA, Germanwala AV, Zanation AM. A controlled laboratory and clinical evaluation of a three-dimensional endoscope for endonasal sinus and skull base surgery. *Am J Rhinol Allergy*. 2011;25(3):141-144.
24. Zaidi HA, Zehri A, Smith TR, Nakaji P, Laws ER Jr. Efficacy of three-dimensional endoscopy for ventral skull base pathology: a systematic review of the literature. *World Neurosurg*. 2016;86:419-431.

25. Cappabianca P, Cavallo LM, Esposito F, de Divitiis E. Endoscopic endonasal transsphenoidal surgery: procedure, endoscopic equipment and instrumentation. *Childs Nerv Syst.* 2004;20(11-12):796-801.
26. Cappabianca P, Alfieri A, Thermes S, Buonamassa S, de Divitiis E. Instruments for endoscopic endonasal transsphenoidal surgery. *Neurosurgery.* 1999;45(2):392-395.
27. Cappabianca P, Cavallo LM, Mariniello G, de Divitiis O, Romero AD, de Divitiis E. Easy sellar reconstruction in endoscopic endonasal transsphenoidal surgery with polyester-silicone dural substitute and fibrin glue: technical note. *Neurosurgery.* 2001;49(2):473-475.
28. Cappabianca P, Esposito F, Esposito I, Cavallo LM, Leone CA. Use of a thrombin-gelatin haemostatic matrix in endoscopic endonasal extended approaches: technical note. *Acta Neurochir (Wien).* 2009;151(1):69-77.
29. Cappabianca P, Esposito F, Magro F, et al. Natura abhorret a vacuo--use of fibrin glue as a filler and sealant in neurosurgical "dead spaces". Technical note. *Acta Neurochir (Wien).* 2010;152(5):897-904.
30. Esposito F, Angileri FF, Kruse P, et al. Fibrin Sealants in Dura Sealing: A Systematic Literature Review. *PLoS One.* 2016;11(4):e0151533.
31. Biroli F, Esposito F, Fusco M, et al. Novel equine collagen-only dural substitute. *Neurosurgery.* 2008;62(3 Suppl 1):273-274.
32. Solari D, Villa A, De Angelis M, Esposito F, Cavallo LM, Cappabianca P. Anatomy and surgery of the endoscopic endonasal approach to the skull base. *Transl Med UniSa.* 2012;2:36-46.
33. Kassam A, Snyderman CH, Mintz A, Gardner P, Carrau RL. Expanded endonasal approach: the rostrocaudal axis. Part I. Crista galli to the sella turcica. *Neurosurg Focus.* 2005;19(1):E3.
34. Kassam A, Snyderman CH, Mintz A, Gardner P, Carrau RL. Expanded endonasal approach: the rostrocaudal axis. Part II. Posterior clinoids to the foramen magnum. *Neurosurg Focus.* 2005;19(1):E4.
35. Cappabianca P, Cavallo LM, Esposito F, de Divitiis O, Messina A, de Divitiis E. Extended endoscopic endonasal approach to the midline skull base: the evolving role of transsphenoidal surgery. *Adv Tech Stand Neurosurg* 2008;33:151–199.
36. Cappabianca P, Frank G, Pasquini E, de Divitiis O, Calbucci F: Extended endoscopic

- endonasal transsphenoidal approach to the suprasellar region, planum sphenoidale and clivus. In de Divitiis E, Cappabianca P (eds): *Endoscopic Endonasal Transsphenoidal Surgery*. Wien, Springer, 2003, pp176-187.
37. Kassam AB, Snyderman C, Gardner P, Carrau R, Spiro R: The expanded endonasal approach: a fully endoscopic transnasal approach and resection of the odontoid process: technical case report. *Neurosurgery*. 2005;57:E213.
 38. Laws ER, Kanter AS, Jane JA, Dumont AS: Extended transphenoidal approach. *J Neurosurg*. 2005;102:825-827.
 39. Messerer M, Maduri R, Daniel RT. Extended endoscopic endonasal approach for craniopharyngioma removal. *J Neurol Surg B Skull Base*. 2018 Feb;79(2):S199-S200.
 40. Alalade AF, Ogando-Rivas E, Boatey J, Souweidane MM, Anand VK, Greenfield JP, Schwartz TH. Suprasellar and recurrent pediatric craniopharyngiomas: expanding indications for the extended endoscopic transsphenoidal approach. *J Neurosurg Pediatr*. 2018;21(1):72-80.
 41. Zada G, Fredrickson VL, Wrobel BB. Extended endoscopic endonasal approach for resection of tuberculum sellae meningioma. *Neurosurg Focus*. 2017 Oct;43(VideoSuppl2):V2.
 42. Castlen JP, Cote DJ, Zaidi HA, Laws ER Jr. The extended, transnasal, transsphenoidal approach for anterior skull base meningioma: considerations in patient selection. *Pituitary*. 2017;20(5):561-568.
 43. Essayed WI, Singh H, Lapadula G, Almodovar-Mercado GJ, Anand VK, Schwartz TH. Endoscopic endonasal approach to the ventral brainstem: anatomical feasibility and surgical limitations. *J Neurosurg*. 2017;127(5):1139-1146.
 44. Zoli M, Rossi N, Friso F, Sturiale C, Frank G, Pasquini E, Mazzatenta D. Limits of endoscopic endonasal approach for cranio-vertebral junction tumors. *J Neurosurg Sci*. 2018 Jan 10. [Epub ahead of print]
 45. Rahme RJ, Arnaout OM, Sanusi OR, Kesavabhotla K, Chandler JP. Endoscopic Approach to Clival Chordomas: The Northwestern Experience. *World Neurosurg*. 2018;110:e231-e238.
 46. Patel CR, Wang EW, Fernandez-Miranda JC, Gardner PA, Snyderman CH. Contralateral transmaxillary corridor: an augmented endoscopic approach to the petrous apex. *J Neurosurg*. 2017;20:1-9.
 47. Cappabianca P, Cavallo LM, Solari D, Di Somma A. Endoscopic transsphenoidal surgery: anatomy, instrumentation and technique. In: Laws ER, Cohen-Gadol AA,

- Schwartz TH, Sheehan JP, eds. *Transsphenoidal Surgery: Complication Avoidance and Management Techniques*. Springer International Publishing; 2017:213-231.
48. Cappabianca P, de Divitiis E. Endoscopy and transsphenoidal surgery. *Neurosurgery*. 2004;54(5):1043-1048.
 49. Hechl PS, Setliff RC, Tschabitscher M. *Endoscopic Anatomy of the Paranasal Sinuses*. Wien: Springer-Verlag; 1997.
 50. Jho HD, Ha HG: Endoscopic endonasal skull base surgery: Part 1—The midline anterior fossa skull base. *Minim Invasive Neurosurg* 2004;47:1–8.
 51. Cavallo LM, de Divitiis O, Aydin S, et al. Extended endoscopic endonasal transsphenoidal approach to the suprasellar area: anatomic considerations—part 1. *Neurosurgery*. 2008;62(6 suppl 3):1202-1212.
 52. Cavallo LM, Messina A, Cappabianca P, Esposito F, de Divitiis E, Gardner P, Tschabitscher M. Endoscopic endonasal surgery of the midline skull base: anatomical study and clinical considerations. *Neurosurg Focus*. 2005;19:E2.
 53. [de Divitiis E](#), [Esposito F](#), [Cappabianca P](#), [Cavallo LM](#), [de Divitiis O](#), [Esposito I](#). Endoscopic transnasal resection of anterior cranial fossa meningiomas. *Neurosurg Focus*. 2008;25(6):E8.
 54. Tschabitscher M, Galzio R: Endoscopic anatomy along the transnasal approach to the pituitary gland and the surrounding structures, in Cappabianca P, de Divitiis E (eds): *Endoscopic Endonasal Transsphenoidal Surgery*. Wien, Springer-Verlag, 2003,pp 21-39.
 55. Bossi Todeschini A, Montaser AS, Hardesty DA, Carrau RL, Prevedello DM. The limits of the endoscopic endonasal transclival approach for posterior fossa tumors. *J Neurosurg Sci*. 2018 Mar 8. [Epub ahead of print].
 56. Kutlay M, Durmaz A, Özer İ, Kural C, Temiz Ç, Kaya S, Solmaz İ, Daneyemez M, Izi Y. Extended endoscopic endonasal approach to the ventral skull base lesions. *Clin Neurol Neurosurg*. 2018 Apr;167:129-140.
 57. Essayed WI, Singh H, Lapadula G, Almodovar-Mercado GJ, Anand VK, Schwartz TH. Endoscopic endonasal approach to the ventral brainstem: anatomical feasibility and surgical limitations. *J Neurosurg*. 2017;127(5):1139-1146.
 58. Cavallo LM, Cappabianca P, Messina A, Esposito F, Stella L, de Divitiis E, Tschabitscher M. The extended endoscopic endonasal approach to the clivus and cranio-vertebral junction: anatomical study. *Childs Nerv Syst*. 2007 Jun;23(6):665-671.

59. Kassam AB, Gardner P, Snyderman C, Mintz A, Carrau R. Expanded endonasal approach: fully endoscopic, completely transnasal approach to the middle third of the clivus, petrous bone, middle cranial fossa, and infratemporal fossa. *Neurosurg Focus*. 2005 Jul 15;19(1):E6.
60. Visocchi M, Iacopino DG, Signorelli F, Olivi A, Maugeri R. Walk the Line. The Surgical Highways to the Craniovertebral Junction in Endoscopic Approaches: A Historical Perspective. *World Neurosurg*. 2018;110:544-557.
61. Fujii T, Platt A, Zada G. Endoscopic Endonasal Approaches to the Craniovertebral Junction: A Systematic Review of the Literature. *J Neurol Surg B Skull Base*. 2015;76(6):480-488.
62. Kshetry VR, Thorp BD, Shriver MF, Zanation AM, Woodard TD, Sindwani R, Recinos PF. Endoscopic Approaches to the Craniovertebral Junction. *Otolaryngol Clin North Am*. 2016;49(1):213-26.
63. Fang CH, Friedman R, Schild SD, Goldstein IM, Baredes S, Liu JK, Eloy JA. Purely endoscopic endonasal surgery of the craniovertebral junction: A systematic review. *Int Forum Allergy Rhinol*. 2015;5(8):754-760.
64. Cappabianca P, Magro F. The lesson of anatomy. *Surg Neurol*. 2009;71(5):597- 598.
65. de Notaris M, Topczewski T, de Angelis M, et al. Anatomic skull base education using advanced neuroimaging techniques. *World Neurosurg*. 2013;79(2 Suppl):S16.e19-13.
66. Chen JC, Amar AP, Levy ML, Apuzzo ML. The development of anatomic art and sciences: the ceroplastica anatomic models of La Specola. *Neurosurgery*. 1999;45(4):883-891.
67. Snyderman C, Kassam A, Carrau R, Mintz A, Gardner P, Prevedello DM. Acquisition of surgical skills for endonasal skull base surgery: a training program. *Laryngoscope*. 2007;117(4):699-705.
68. Evans CH, Schenarts KD. Evolving Educational Techniques in Surgical Training. *Surg Clin North Am*. 2016;96(1):71-88.
69. Bernardo A. Virtual Reality and Simulation in Neurosurgical Training. *World Neurosurg*. 2017;106:1015-1029.
70. Urgun K, Toktas ZO, Akakin A, Yilmaz B, Sahin S, Kilic T. A Very Quickly Prepared, Colored Silicone Material for Injecting into Cerebral Vasculature for Anatomical Dissection: A Novel and Suitable Material for both Fresh and Non-Fresh Cadavers. *Turk Neurosurg*. 2016;26(4):568-573.

71. Ganju A, Aoun SG, Daou MR, et al. The role of simulation in neurosurgical education: a survey of 99 United States neurosurgery program directors. *World Neurosurg.* 2013;80(5):e1-8.
72. Moon K, Filis AK, Cohen AR. The birth and evolution of neuroscience through cadaveric dissection. *Neurosurgery.* 2010;67(3):799-809; discussion 809-710.
73. Holland JP, Waugh L, Horgan A, Paleri V, Deehan DJ. Cadaveric hands-on training for surgical specialties: is this back to the future for surgical skills development? *J Surg Educ.* 2011;68(2):110-116.
74. Bernardo A, Preul MC, Zabramski JM, Spetzler RF. A three-dimensional interactive virtual dissection model to simulate transpetrous surgical avenues. *Neurosurgery.* 2003;52(3):499-505.
75. de Notaris M, Palma K, Serra L, et al. A three-dimensional computer-based perspective of the skull base. *World Neurosurg.* 2014;82(6 Suppl):S41-48.
76. de Notaris M, Prats-Galino A, Cavallo LM, et al. Preliminary experience with a new three-dimensional computer-based model for the study and the analysis of skull base approaches. *Childs Nerv Syst.* 2010;26(5):621-626.
77. de Notaris M, Prats-Galino A, Enseñat J, et al. Quantitative analysis of progressive removal of nasal structures during endoscopic suprasellar approach. *Laryngoscope.* 2014;124(10):2231-2237.
78. de Notaris M, Solari D, Cavallo LM, et al. The use of a three-dimensional novel computer-based model for analysis of the endonasal endoscopic approach to the midline skull base. *World Neurosurg.* 2011;75(1):106-113; discussion 136-140.
79. Hakuba A, Tanaka K, Suzuki T, Nishimura S. A combined orbitozygomatic infratemporal epidural and subdural approach for lesions involving the entire cavernous sinus. *J Neurosurg.* 1989;71(5 Pt 1):699-704.
80. Gonzalez LF, Crawford NR, Horgan MA, Deshmukh P, Zabramski JM, Spetzler RF. Working area and angle of attack in three cranial base approaches: pterional, orbitozygomatic, and maxillary extension of the orbitozygomatic approach. *Neurosurgery.* 2002;50(3):550-555.
81. Perneczky A, Fries G. Endoscope-assisted brain surgery: part 1--evolution, basic concept, and current technique. *Neurosurgery.* 1998;42(2):219-224.
82. Reisch R, Perneczky A, Filippi R. Surgical technique of the supraorbital key-hole craniotomy. *Surg Neurol.* 2003;59(3):223-227.

83. Prosser JD, Figueroa R, Carrau RI, Ong YK, Solares CA. Quantitative analysis of endoscopic endonasal approaches to the infratemporal fossa. *Laryngoscope*. 2011;121(8):1601-1605.
84. de Notaris M, Prats-Galino A. Surgical freedom: a challenging topic in endoscopic endonasal approaches. *World Neurosurg*. 2014;82(1-2):e387-388.
85. Wilson DA, Williamson RW, Preul MC, Little AS. Comparative analysis of surgical freedom and angle of attack of two minimal-access endoscopic transmaxillary approaches to the anterolateral skull base. *World Neurosurg*. 2014;82(3-4):e487-493.
86. Dallan I, Lenzi R, de Notaris M, et al. Quantitative study on endoscopic endonasal approach to the posterior sino-orbito-cranial interface: implications and clinical considerations. *Eur Arch Otorhinolaryngol*. 2014;271(8):2197-2203.
87. de Notaris M, Cavallo LM, Prats-Galino A, et al. Endoscopic endonasal transclival approach and retrosigmoid approach to the clival and petroclival regions. *Neurosurgery*. 2009;65(6 Suppl):42-50.
88. Solari D, Cappabianca P. Far medial versus far lateral approach: the need of a chamaleontic perspective to unlock a skull base region. *World Neurosurg*. 2014;81(2):279-280.
89. Di Somma A, de Notaris M, Stagno V, et al. Extended endoscopic endonasal approaches for cerebral aneurysms: anatomical, virtual reality and morphometric study. *Biomed Res Int*. 2014;2014:703792.
90. Bernardo A, Evins AI, Mattogno PP, Quiroga M, Zacharia BE. The Orbit as Seen Through Different Surgical Windows: Extensive Anatomical Study. *World Neurosurg*. 2017;106:1030-1046.
91. [Chowdhury FH](#), [Haque MR](#), [Kawsar KA](#), [Ara S](#), [Mohammad QD](#), [Sarker MH](#), [Goel AH](#). Endoscopic endonasal transsphenoidal exposure of circle of Willis (CW); can it be applied in vascular neurosurgery in the near future? A cadaveric study of 26 cases. *Turk Neurosurg* 2012;22(1):68-76.
92. Ensenat J, Alobid I, de Notaris M, Sanchez M, Valero R, Prats-Galino A, Ferre E. Endoscopic endonasal clipping of a ruptured vertebral-posterior inferior cerebellar artery aneurysm: technical case report. *Neurosurgery* 2011;69:onsE121-27.
93. Froelich S, Cebula H, Debry C, Boyer P. [Anterior communicating artery aneurysm clipped via an endoscopic endonasal approach: technical note](#). *Neurosurgery* 2011 Jun;68(2 Suppl Operative):310-316.

94. Germanwala AV, Zanation AM. Endoscopic endonasal approach for clipping of ruptured and unruptured paraclinoid cerebral aneurysms: case report. *Neurosurgery* 2011;68:234-239.
95. Kassam AB, Gardner PA, Mintz A, Snyderman CH, Carrau RL, Horowitz M. Endoscopic endonasal clipping of an unsecured superior hypophyseal artery aneurysm. Technical note. *J Neurosurg.* 2007;107(5):1047-1052.
96. Kassam AB, Mintz AH, Gardner PA, Horowitz MB, Carrau RL, Snyderman CH. The expanded endonasal approach for an endoscopic transnasal clipping and aneurysmorrhaphy of a large vertebral artery aneurysm: technical case report. *Neurosurgery.* 2006;59(1 suppl 1):162-165.
97. Kitano M, Taneda M. Extended transsphenoidal approach to anterior communicating artery aneurysm: aneurysm incidentally identified during macroadenoma resection: technical case report. *Neurosurgery.* 2007;61(5 suppl 2):299-300.
98. Ruggeri A, Enseñat J, Prats-Galino A, Lopez-Rueda A, Berenguer J, Cappelletti M, De Notaris M, d'Avella E. Endoscopic endonasal control of the paraclival internal carotid artery by Fogarty balloon catheter inflation: an anatomical study. *J Neurosurg.* 2017 Mar;126(3):872-879.
99. Enseñat J, d'Avella E, Tercero A, Valero R, Alobid I. Endoscopic endonasal surgery for a mesencephalic cavernoma. *Acta Neurochir (Wien).* 2015;157(1):53-55.
100. Sekhar LN, Farzana T, Morton RP, Ghodke B, Hallam DK, Marber J, Kim LJ: Basilar tip aneurysms: a microsurgical and endovascular contemporary series of 100 patients. *Neurosurgery.* 2013; 72: 284-298.
101. Henkes H, Fischer S, Mariushi W, Weber W, Liebig T, Miloslavski E, Brew S, Kühne D: Angiographic and clinical results in 316 coil- treated basilar artery bifurcation aneurysms. *J Neurosurg.* 2005; 103:990-999.
102. Kallmes DF, Hanel R, Lopes D, Boccardi E, Bonafé A, Cekirge S, Fiorella D, Jabbour P, Levy E, McDougall C, Siddiqui A, Szikora I, Woo H, Albuquerque F, Bozorgchami H, Dashti SR, Delgado Almandoz JE, Kelly ME, Turner IV R, Woodward BK, Brinjikji W, Lanzino G, Lylyk P: International retrospective study of the pipeline embolization device: a multicenter aneurysm treatment study. *AJNR Am J Neuroradiol.* 2015; 36:108-115.

103. Pandey AS, Koebbe C, Rosenwasser RH, Veznedaroglu E: Endovascular coil embolization of ruptured and unruptured posterior circulation aneurysms: review of a 10-year experience. *Neurosurgery*. 2007; 60:626-636.
104. Mordasini P, Schroth G, Guzman R, Barth A, Seiler RW, Remonda L. Endovascular treatment of posterior circulation cerebral aneurysms by using Guglielmi detachable coils: a 10-year single-center experience with special regard to technical development. *AJNR Am J Neuroradiol*. 2005; 26(7):1732-1738.
105. Viñuela F, Duckwiler G, Mawad M. Guglielmi detachable coil embolization of acute intracranial aneurysm: perioperative anatomical and clinical outcome in 403 patients. *J Neurosurg*. 1997; 86(3):475-482.
106. Thorell WE, Chow MM, Woo HH, Masaryk TJ, Rasmussen PA. Y-configured dual intracranial stent-assisted coil embolization for the treatment of wide-necked basilar tip aneurysms. *Neurosurgery*. 2005; 56(5):1035-1040; discussion 1035-1040.
107. Kulcsár Z, Ernemann U, Wetzel SG, et al. High-profile flow diverter (silk) implantation in the basilar artery: efficacy in the treatment of aneurysms and the role of the perforators. *Stroke*. 2010; 41(8):1690-1696.
108. Fiorella D, Albuquerque FC, Masaryk TJ, Rasmussen PA, McDougall CG. Balloon-in-stent technique for the constructive endovascular treatment of “ultra- wide necked” circumferential aneurysms. *Neurosurgery*. 2005; 57(6):1218-1227; discussion 1218-1227.
109. Chow MM, Woo HH, Masaryk TJ, Rasmussen PA. A novel endovascular treatment of a wide-necked basilar apex aneurysm by using a Y-configuration, double-stent technique. *AJNR Am J Neuroradiol*. 2004; 25(3):509-512.
110. Nagashima H, Kobayashi S, Tanaka Y, Hongo K. Endovascular therapy versus surgical clipping for basilar artery bifurcation aneurysm: retrospective analysis of 117 cases. *J Clin Neurosci*. 2004;11(5):475-479.
111. Henkes H, Fischer S, Mariushi W, et al. Angiographic and clinical results in 316 coil-treated basilar artery bifurcation aneurysms. *J Neurosurg*. 2005;103(6): 990-999.
112. Chalouhi N, Jabbour P, Gonzalez LF, et al. Safety and efficacy of endovascular treatment of basilar tip aneurysms by coiling with and without stent assistance: a review of 235 cases. *Neurosurgery*. 2012; 71(4):785-794.

113. Tjahjadi M1, Kivelev J, Serrone JC, Maekawa H, Kerro O, Jahromi BR, Lehto H, Niemelä M, Hernesniemi JA. Factors Determining Surgical Approaches to Basilar Bifurcation Aneurysms and Its Surgical Outcomes. *Neurosurgery*. 2016;78(2):181-191
114. Drake CG , Peerless SJ , Hernesniemi J : A:Surgery of Vertebrobasilar Aneurysms. London, Ontario Experience on 1767 Patients. Vienna: Springer-Verlag 1996; 21-26.
115. Hernesniemi J, Ishii K, Niemelä M, Kivipelto L, Fujiki M, Shen H: Subtemporal approach to basilar bifurcation aneurysms: advanced technique and clinical experience. *Acta Neurochir*. 2005; 94(Suppl 1):31-38.
116. McLaughlin N, Martin NA: Extended subtemporal transtentorial approach to the anterior incisural space and upper clival region: experience with posterior circulation aneurysms. *Neurosurgery* 2014; 10(Suppl 1):15-23.
117. Hernesniemi J, Goehre F. Approaches to upper basilar artery aneurysms. *World Neurosurg*. 2014 Dec; 82(6):1001-2.
118. Kakino S, Ogasawara K, Kubo Y, Nishimoto H, Ogawa A: Subtemporal approach to basilar tip aneurysm with division of posterior communicating artery: technical note. *Vasc Health Risk Manag* 2008; 4:931-935.
119. Hernesniemi J, Ishii K, Karatas A, Kivipelto L, Niemelä M, Nagy L, Shen H: Surgical technique to retract the tentorial edge during subtemporal approach: technical note. *Neurosurgery* 2005; 57(Suppl 4):E408 .
120. Yasargil MG, Antic J, Laciga R, Jain KK, Hodosh RM, Smith RD: Microsurgical pterional approach to aneurysms of the basilar bifurcation. *Surg Neurol* 1976; 6:83-91.
121. Heros RC, Lee SH: The combined pterional/ anterior temporal approach for aneurysms of the upper basilar complex: technical report. *Neurosurgery* 1993; 33:244-251.
122. Nutik SL. Pterional craniotomy via a transcavernous approach for the treatment of low-lying distal basilar artery aneurysms. *J Neurosurg*. 1998; 89(6):921-926.
123. Lawton MT. Basilar artery bifurcation aneurysm. In: Lawton MT, ed. *Seven Aneurysms: Tenets and Techniques for Clipping*. New York, NY: Thieme; 2011: 164-192.

124. Yasargil MG. Vertebrobasilar aneurysms. In: Yasargil MG, ed. *Microneurosurgery: Clinical Considerations, Surgery of the Intracranial Aneurysms and Result*. Vol. 2. New York, NY: Thieme, 1984: 232-256.
125. Nanda A, Sonig A, Banerjee AD, Javalkar VK. Microsurgical management of basilar artery Apex aneurysms: a single Surgeon's experience from Louisiana State University, Shreveport. *World Neurosurg*. 2014; 82(1-2):118-129.
126. Krisht AF, Kadri PA: Surgical clipping of complex basilar apex aneurysms: a strategy for successful outcome using the pretemporal transzygomatic transcavernous approach. *Neurosurgery* 2005;56: 261-273; discussion 273.
127. Krisht AF, Krayenbuhl N, Sercl D, Bikmaz K, Kadri PA: Results of microsurgical clipping of 50 high complexity basilar apex aneurysms. *Neurosurgery* 2007; 60:242-250; discussion 250-252.
128. Chanda A, Nanda A: Anatomical study of the orbitozygomatic transsellar-transcavernous-transclinoidal approach to the basilar artery bifurcation. *J Neurosurg* 2002; 97:151–160.
129. Day JD, Giannotta SL, Fukushima T: Extradural temporopolar approach to lesions of the upper basilar artery and infrachiasmatic region. *J Neurosurg* 1994; 81:230–235.
130. Dolenc VV, Skrap M, Sustersic J, Skrbec M, Morina A. A transcavernous-transsellar approach to the basilar tip aneurysms. *Br J Neurosurg*. 1987; 1(2): 251-259.
131. Seoane E, Tedeschi H, de Oliveira E, Wen HT, Rhoton AL Jr. The pretemporal transcavernous approach to the interpeduncular and prepontine cisterns: microsurgical anatomy and technique application. *Neurosurgery* 2000;46(4): 891-898.
132. Figueiredo EG, Zabramski JM, Deshmukh P, Crawford NR, Preul MC, Spetzler RF. Anatomical and quantitative description of the transcavernous approach to interpeduncular and prepontine cisterns: technical note. *J Neurosurg*. 2006; 104(6):957-964.
133. Gonzalez LF, Amin-Hanjani S, Bambakidis NC, Spetzler RF. Skull base approaches to the basilar artery. *Neurosurg Focus*. 2005; 19(5):E3.
134. Hsu FP, Clatterbuck RE, Spetzler RF. Orbitozygomatic approach to basilar apex aneurysms. *Neurosurgery*. 2005; 56(1 suppl):172-177; discussion 172-177.

135. Basma JI, Ryttefors M, Latini F, Pravdenkova S, Krisht A. Mobilization of the trans cavernous oculomotor nerve during basilar aneurysm surgery: biomechanical bases for better outcome. *Neurosurgery*. 2014 Mar;10 Suppl 1:106-14.
136. Hernesniemi J, Ishii K, Niemelä M, Smrcka M, Kivipelto L, Fujiki M, Shen H. Lateral supraorbital approach as an alternative to the classical pterional approach. *Acta Neurochir Suppl*. 2005;94: 17-21.
137. Drazin D, Zhuang L, Schievink WI, Mamelak AN: Expanded endonasal approach for the clipping of a ruptured basilar aneurysm and feeding artery to a cerebellar arteriovenous malformation. *J Clin Neurosci* 2012; 19:144-148.
138. Kassam AB, Prevedello DM, Thomas A, Gardner P, Mintz A, Snyderman C, Carrau R: Endoscopic endonasal pituitary transposition for a transdorsum sellae approach to the interpeduncular cistern. *Neurosurgery* 2008; 62:57-72; discussion 74.
139. Gardner PA, Vaz-Guimaraes F, Jankowitz B, Koutourosiou M, Fernandez-Miranda JC, Wang EW, Snyderman CH. Endoscopic Endonasal Clipping of Intracranial Aneurysms: Surgical Technique and Results. *World Neurosurg*. 2015 Nov; 84(5):1380-93.
140. Szentirmai O, Hong Y, Mascarenhas L, Salek AA, Stieg PE, Anand VK, Cohen-Gadol AA, Schwartz TH. Endoscopic endonasal clip ligation of cerebral aneurysms: an anatomical feasibility study and future directions. *Neurosurgery*. 2005 Apr; 56(2 Suppl):274-80; discussion 274-80.
141. Kassam A, Snyderman CH, Carrau RL, Gardner P, Mintz A: Endoneurosurgical hemostasis techniques: lessons learned from 400 cases. *Neurosurg Focus* 2005; 19:E7.
142. Drazin D, Zhuang L, Schievink WI, Mamelak AN: Expanded endonasal approach for the clipping of a ruptured basilar aneurysm and feeding artery to a cerebellar arteriovenous malformation. *J Clin Neurosci* 2012; 19(1):144–148.
143. Somanna S, Babu RA, Srinivas D, Narasinga Rao KV, Vazhayil V. Extended endoscopic endonasal transclival clipping of posterior circulation aneurysms--an alternative to the transcranial approach. *Acta Neurochir (Wien)*. 2015 Dec; 157(12):2077-85.
144. Labib M, Dehdashti AR. Extended endoscopic endonasal transclival clipping of posterior circulation aneurysms-an alternative to the transcranial approach. *Acta Neurochir (Wien)*. 2015 Dec; 157(12):2087-8.

145. Kalavakonda C, Sekhar LN, Ramachandran P, Hechl P. Endoscope-assisted microsurgery for intracranial aneurysms. *Neurosurgery* 2002; 51:1119-26. 4.
146. Matula C, Tschabitscher M, Day JD, Reinprecht A, Koos WT. Endoscopically assisted microneurosurgery. *Acta Neurochir (Wien)* 1995; 134:190-5.
147. Fries G, Perneczky A. Endoscope-Assisted Keyhole Surgery for Aneurysms of the Anterior Circulation and the Basilar Apex. *Operative Techniques in Neurosurgery*, Vol 3, No 4 (December), 2000: pp 216-230.
148. Filipce V, Ammirati M. Quantitative and qualitative analysis of the working area obtained by endoscope and microscope in pterional and orbitozygomatic approach to the basilar artery bifurcation using computed tomography based frameless stereotaxy: A cadaver study. *Asian J Neurosurg* 2015; 10:69-74.
149. Lai LT, Morgan MK, Chin DC, Snidvongs K, Huang JX, Malek J, Lam M, McLachlan R, Harvey RJ: A cadaveric study of the endoscopic endonasal transclival approach to the basilar artery. *J Clin Neurosci* 2013; 20(4):587–592
150. Youssef AS, Abdel Aziz KM, Kim EY, Keller JT, Zuccarello M, van Loveren HR. The carotid-oculomotor window in exposure of upper basilar artery aneurysms: a cadaveric morphometric study. *Neurosurgery* 2004; 54(5):1181-1187.
151. Sanai N, Tarapore P, Lee AC, Lawton MT. The current role of microsurgery for posterior circulation aneurysms: a selective approach in the endovascular era. *Neurosurgery* 2008; 62(6):1236-1249.
152. Abla AA, Lawton MT, Spetzler RF. The art of basilar apex aneurysm surgery: is it sustainable in the future? *World Neurosurg* 2014; 82(1-2):e51-e53.
153. Sekhar LN, Tariq F, Osbun J. Far lateral and far medial approaches to the foramen magnum: microsurgery or endoscopy? *World Neurosurg.* 2014;81(2):283-4.
154. Schwartz TH. The high road or the low road. *World Neurosurg.* 2014;81(2):281-282.
155. Benet A, Prevedello DM, Carrau RL, Rincon-Torroella J, Fernandez-Miranda JC, Prats-Galino A, Kassam AB. Comparative analysis of the transcranial "far lateral" and endoscopic endonasal "far medial" approaches: surgical anatomy and clinical illustration. *World Neurosurg.* 2014;81(2):385-396.
156. Dehdashti AR, Karabatsou K, Ganna A, Witterick I, Gentili F. Expanded endoscopic endonasal approach for treatment of clival chordomas: early results in 12 patients. *Neurosurgery.* 2008 Aug;63(2):299-307.

Figures

Figure 1. Cadaveric dissection showing the exposure of the sellar dura and left paraclival internal carotid artery (ICA) through an endoscopic endonasal parasепtal approach. A Fogarty balloon catheter is approximated to the bony opening and inserted extradurally and extra-arterially along the paraclival ICA. The catheter is then pushed posteriorly and laterally toward the foramen lacerum until it naturally stops. F = Fogarty balloon catheter; GF = grasping forceps; IICAp = left paraclival ICA; PG = pituitary gland; PS = planum sphenoidale; TS = tuberculum sellae.

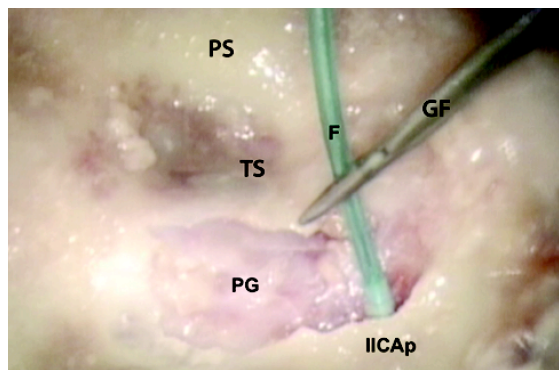


Figure 2. CT scan (bone window, axial slices) showing the ICA course from the intrapetrous to the paraclival segment with a clockwise caudo-cranial progression. At the level of the left paraclival ICA, the metallic core of the distal end of the Fogarty catheter (left) and the balloon after inflation (right) are visible (red arrows).

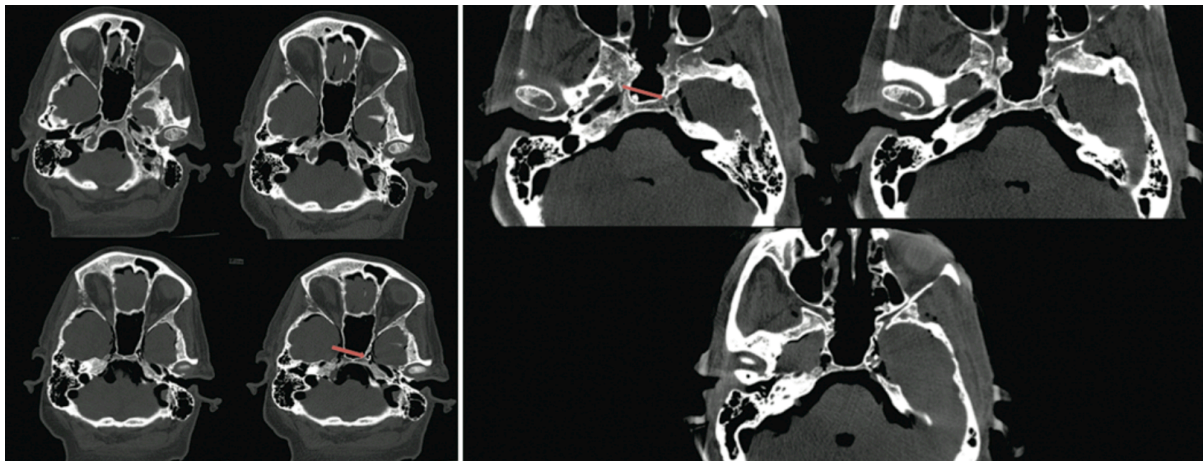


Figure 3. Anterior (right) and lateral (left) cerebral angiograms of the left ICA. Clockwise, the images show the interruption of contrast flow when the Fogarty catheter balloon is inflated at the level of the paraclival ICA, and the progressive passage of contrast as the balloon is deflated.

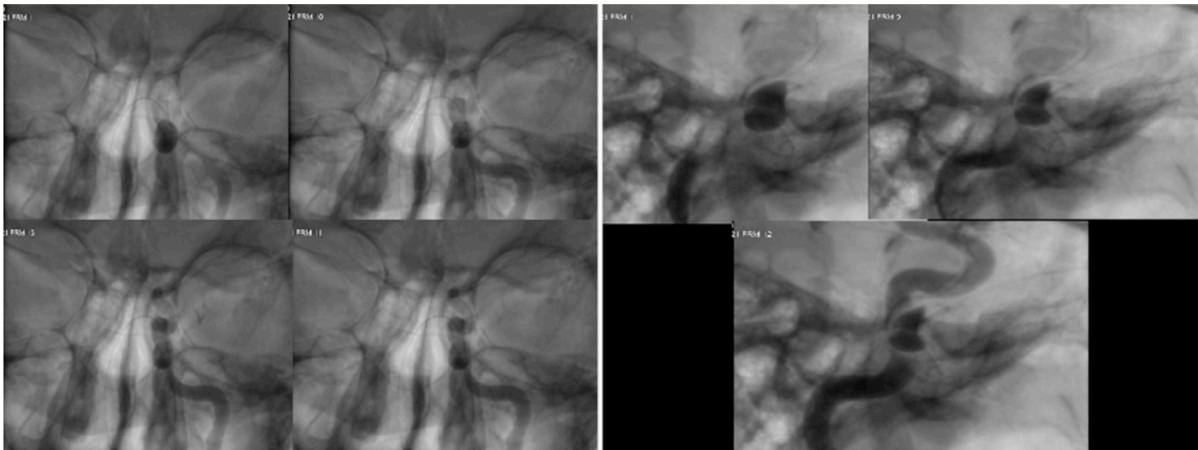


Figure 4. A: Magnetic resonance image showing a right macroadenoma with cavernous sinus invasion. The patient underwent endoscopic endonasal surgery. B: The parasепtal approach was performed. The pituitary adenoma and right paraclival ICA were exposed. C: A Fogarty balloon catheter was inserted extra-arterially and extradurally along the paraclival ICA until it naturally stopped. D: The catheter was left in situ to be inflated in case of intraoperative ICA rupture. a = aspirator; d = dissector; F = Fogarty balloon catheter; PitAdenoma = pituitary adenoma; rICAp = right paraclival ICA.

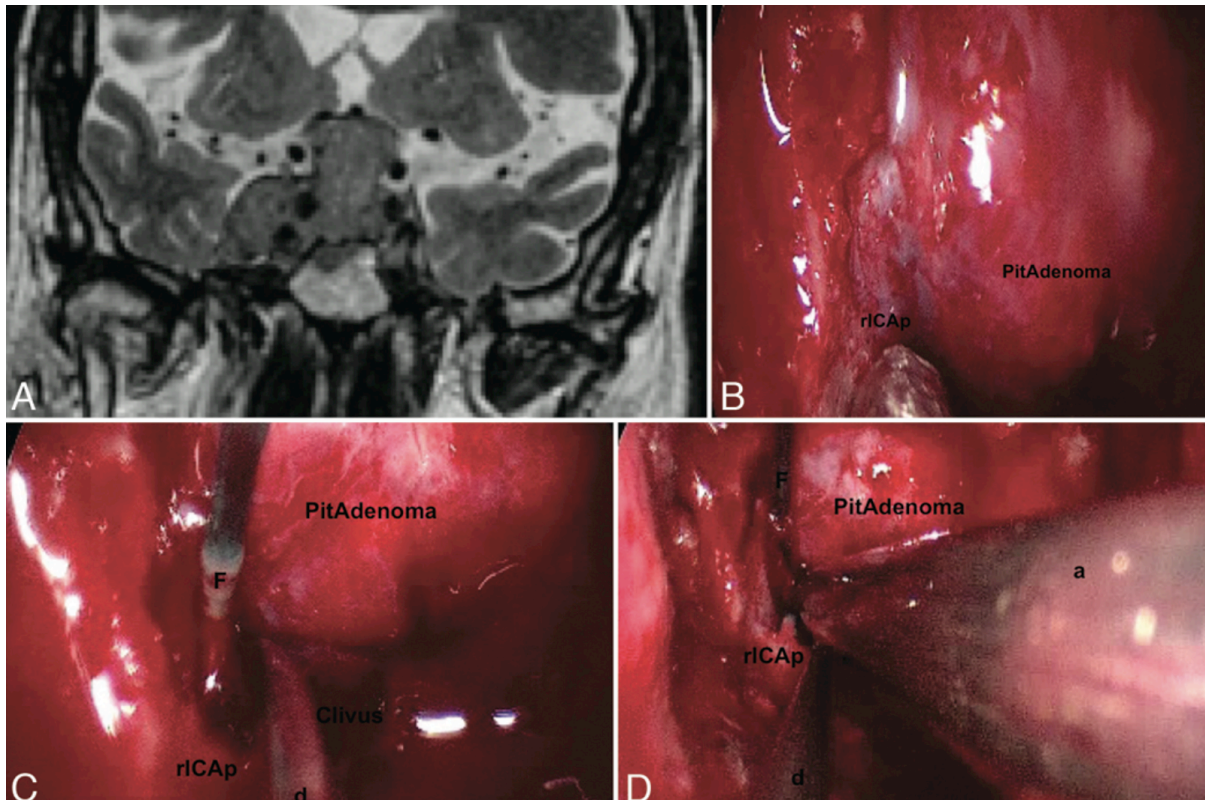


Figure 5. A 3D reconstruction of the endoscopic endonasal parasепtal approach was obtained with Amira (Amira Visage Imaging Inc.), a specific software program for the visualization and manipulation of biomedical data. A: Bone removal at the sellar floor and the paraclival ICA protuberance with visualization of the pituitary gland (purple), left paraclival ICA (red), and Fogarty balloon (blue) catheter (green). B: Localization of the Fogarty balloon catheter compressing the left ICA. C: The left ICA is compressed and occluded by the Fogarty balloon.

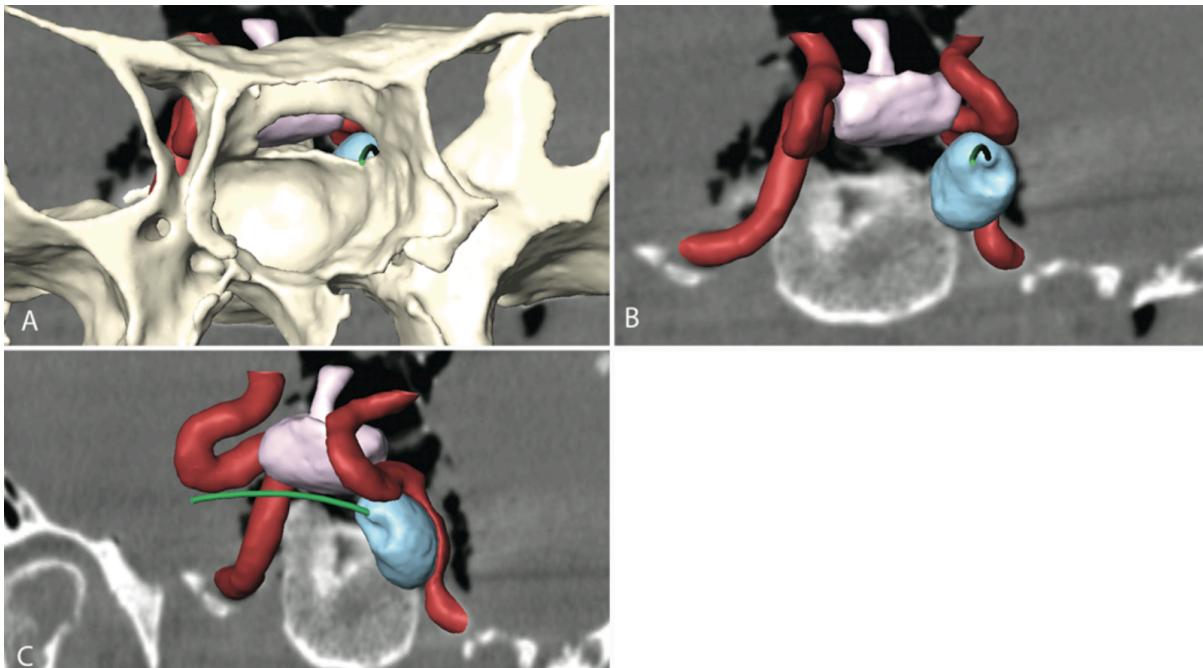


Figure 6. T1-weighted post-contrast magnetic resonance image demonstrating a cavernoma surfacing at the ventromedial mesencephalon (a). Intra-operative images of the extended endoscopic endonasal transplanum transtuberculum approach to the mesencephalic cavernoma. The hematoma overlying the cavernous malformation was encountered on the ventral surface of the midbrain, pushing forward the basilar artery and the perforators, creating itself the space for surgical maneuvers (b). Once the hematoma was evacuated and the cavernoma removed, the basilar artery and perforators fell onto the mesencephalic ventral surface, obliterating the corridor to the surgical cavity and making it too risky for any other inspection of the cavernoma's bed (c). Post-operative axial T1-weighted magnetic resonance imaging demonstrating resection of the lesion with small fragments of the cavernoma in the surgical cavity (d). CP right cerebral peduncle, MB mammillary bodies, C cavernoma, BA basilar artery.

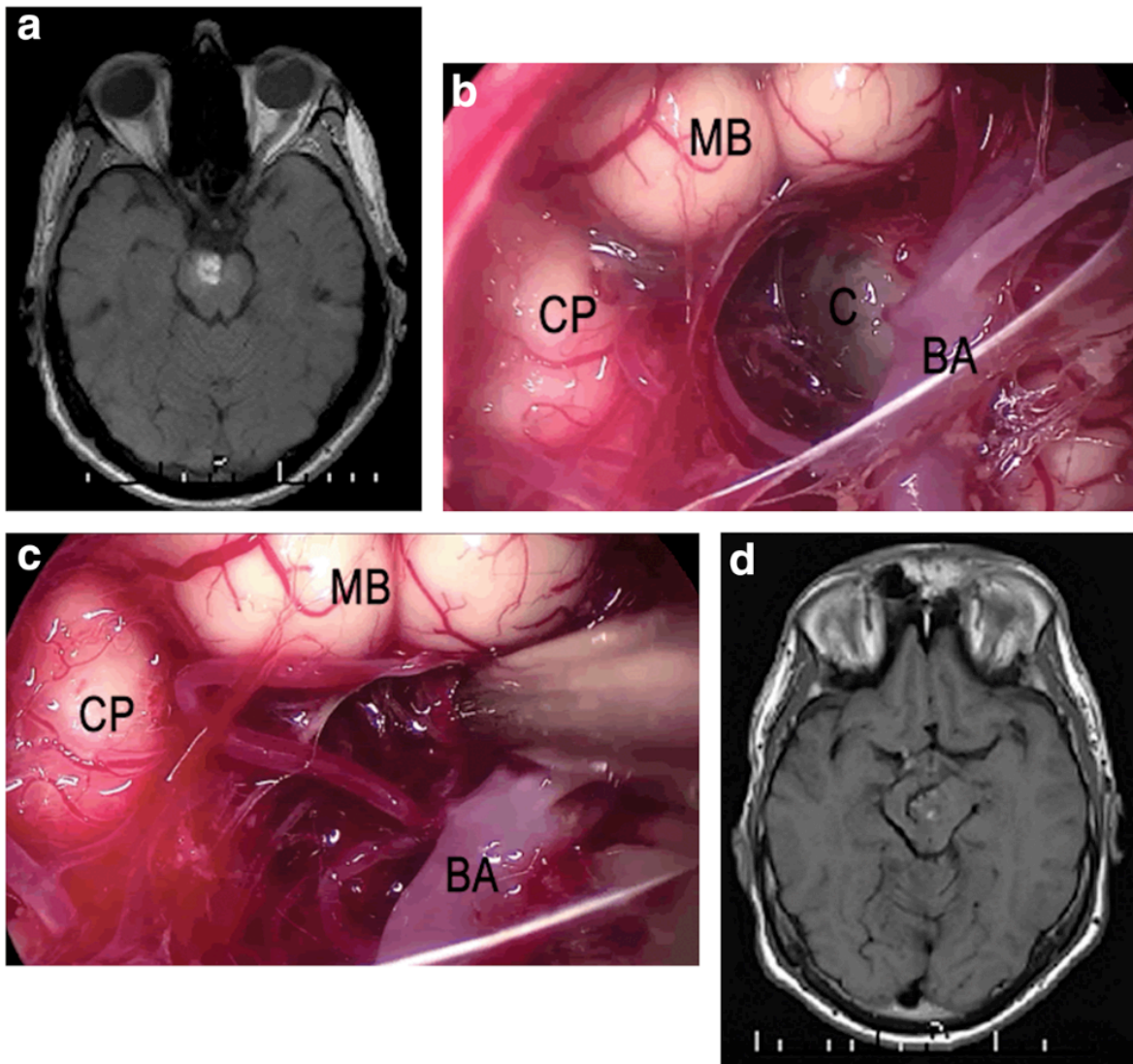
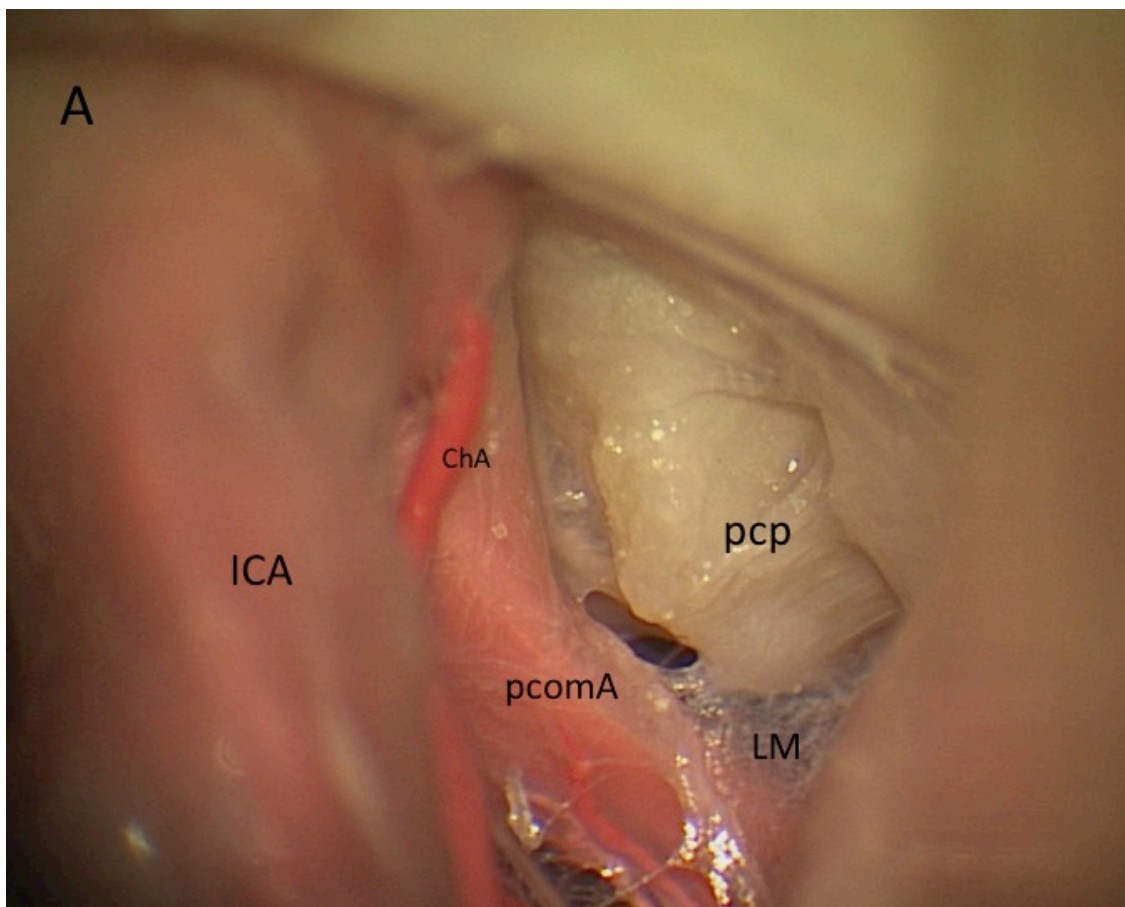


Figure 7. The basilar apex in the interpeduncular cistern was reached via the lateral supraorbital approach through a corridor between the right oculomotor nerve and the right internal carotid artery (ICA) by microsurgical dissection in a medio-lateral direction, until the posterior communicating artery (pcomA) was identified (A). The pcomA was followed along the inferior surface of the temporal lobe to its origin from the posterior cerebral artery. The supraclinoid tract of the ICA was medially withdrawn together with PcomA, to increase visibility through the oculomotor-carotid corridor. After opening of the Lilequist membrane, the interpeduncular cistern is reached. In the depth of the field, the pre-communicating segment of the posterior cerebral artery and the basilar tip can be seen, although the posterior clinoid process limits anatomical exposure (B). ICA: internal carotid artery; pcp: posterior clinoid process; pcomA: posterior communicating artery; LM: Lilequist membrane; ChA: choroidal artery; IICN: third cranial nerve; BA: basilar apex; PCA: posterior cerebral artery.



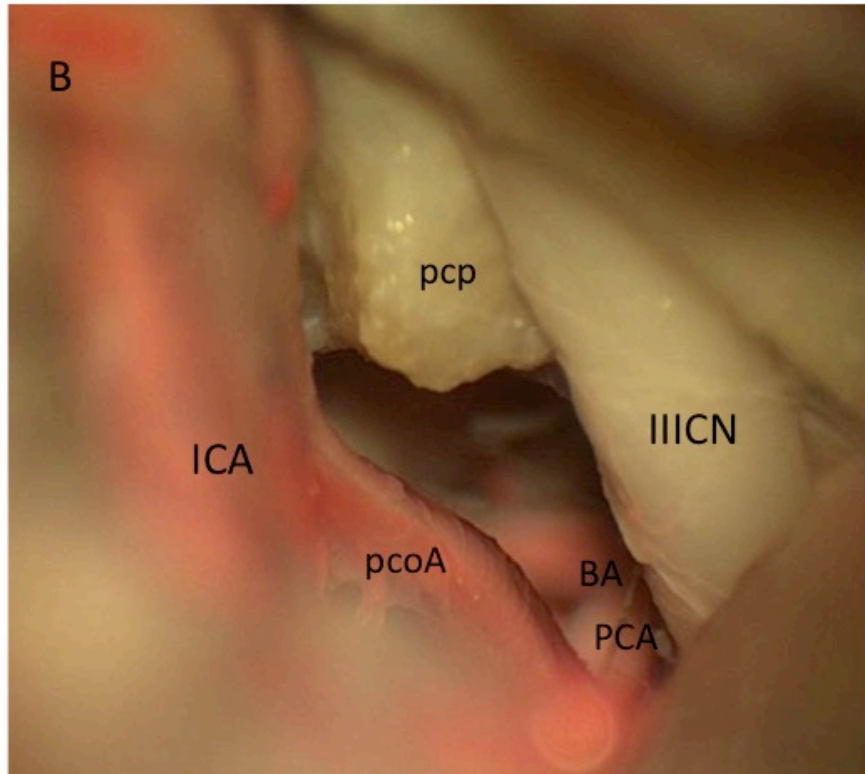


Figure 8. Through a lateral supraorbital approach, lateral to the oculomotor nerve, the right superior cerebellar artery running along the tentorial edge can be seen. TE: tentorial edge; SCA: superior cerebellar artery; IICN: third cranial nerve; pcoA: posterior communicating artery.

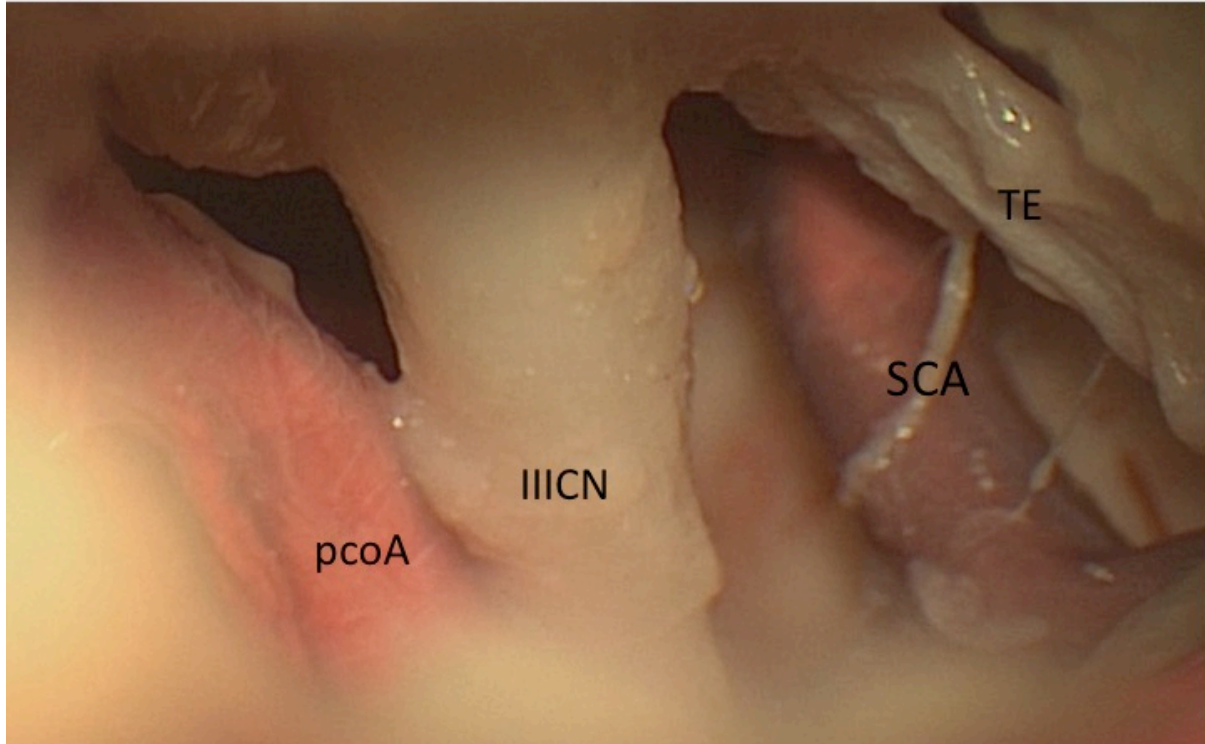


Figure 9. After posterior clinoidectomy, endoscopic assistance allows for a wider anatomical exposure around the basilar apex: the basilar trunk becomes visible for 7,4 mm ($\pm 3,7$ mm), superior cerebellar artery (SCA) is exposed for 9,6 mm ($\pm 5,2$ mm) ipsilaterally and for 3,9 mm ($\pm 2,8$ mm) contralaterally; posterior cerebral arteries are exposed for 6,2 mm ($\pm 4,3$ mm) contralaterally and for 11,4 mm ($\pm 2,6$ mm) ipsilaterally.

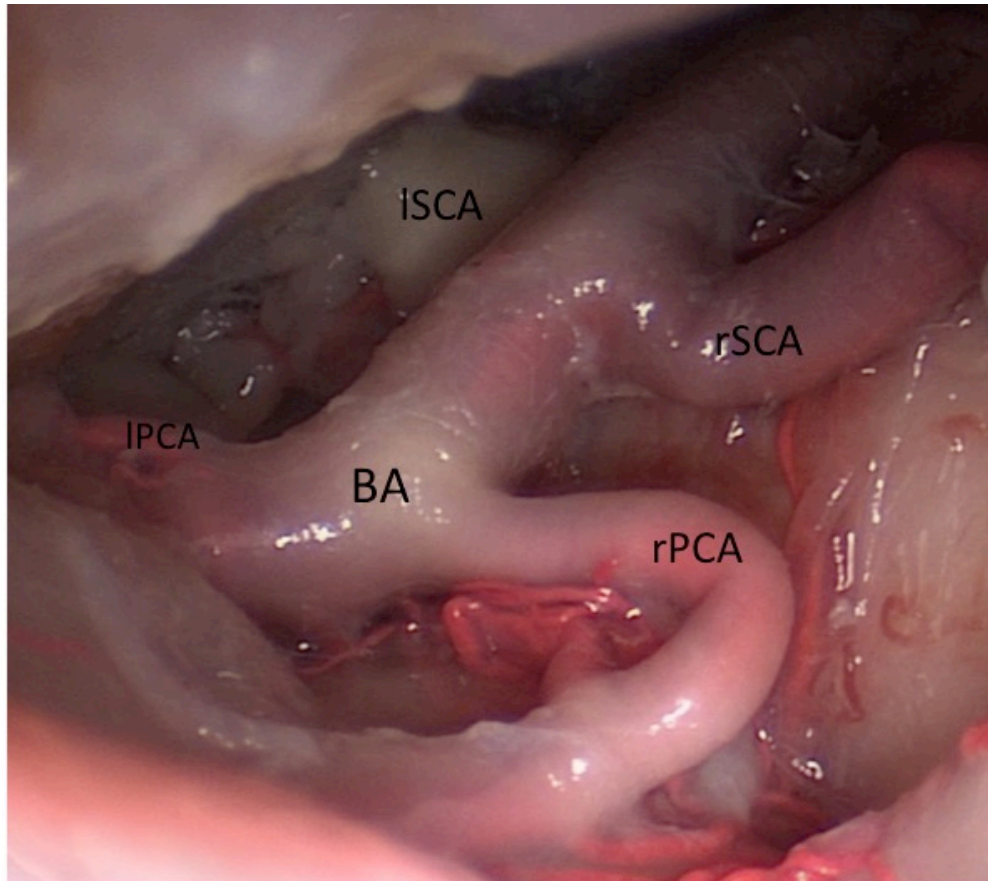


Figure 10. The endoscopic endonasal transclival approach is performed by drilling of the clival bone from the floor of the sella inferiorly to 2/3 of the clivus (A). Then dura is opened on the midline and prepontine cistern and vessels inside it are exposed free from arachnoid (B).

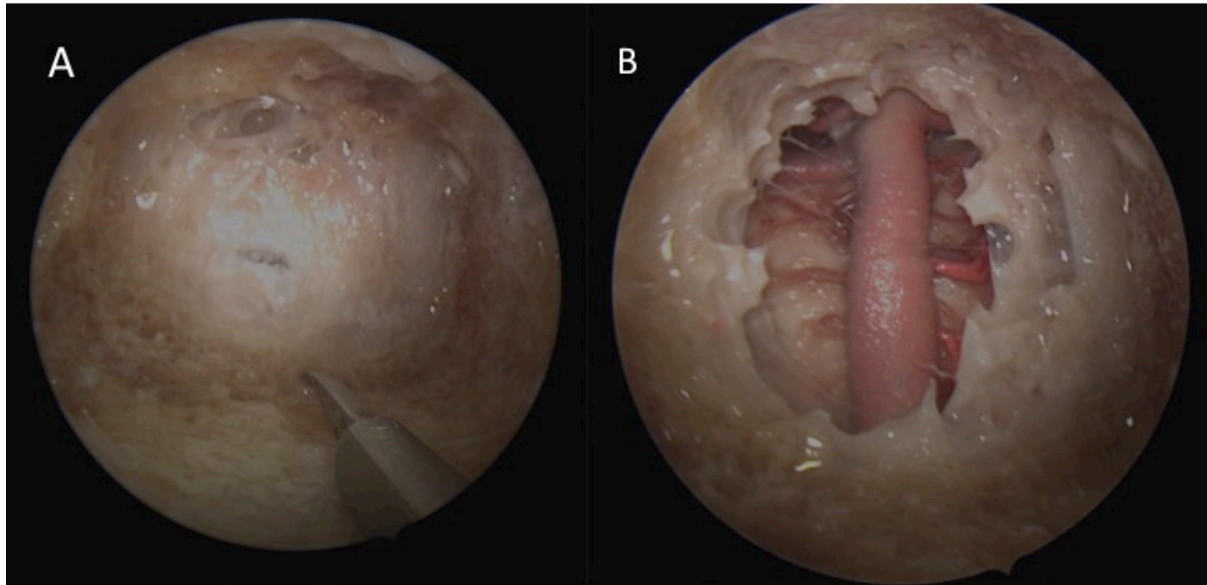


Figure 11. Anatomical exposure and surgical freedom around the basilar apex as provided by the lateral supraorbital approach were measured before (A) and after (B) posterior clinoidectomy. Posterior clinoidectomy increased surgical freedom up to 54,3 mm²; anatomical exposure expanded inferiorly and controlaterally: basilar trunk became visible for 4,6 mm (\pm 2,8 mm) caudally from its apex, controlateral posterior cerebral artery was exposed for 6,2 mm (\pm 4,3 mm), while ipsilateral exposure remained unchanged. BA: basilar artery; rPCA: right posterior cerebral artery; lPCA: left posterior cerebral artery.

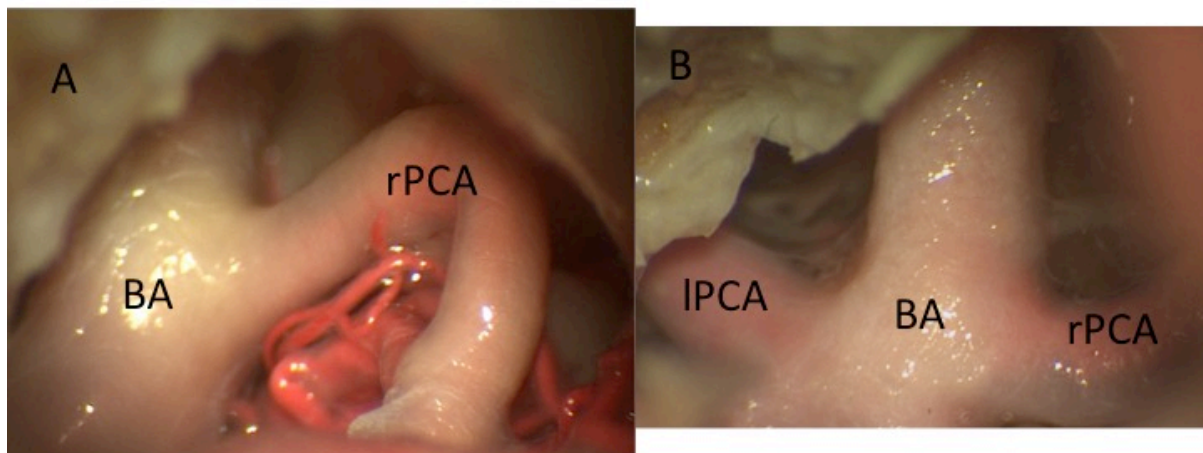


Figure 12. Surgical freedom and anatomical exposure are increased by drilling of dorsum sellae during an endoscopic endonasal transclival approach. After this maneuver, surgical freedom measures $101,3\text{mm}^2(\pm 23,6\text{mm}^2)$; posterior cerebral arteries can be exposed for $5\text{mm}(\pm 2,7\text{mm})$ on average bilaterally; exposure of basilar trunk increases for $3,4\text{mm}(\pm 4,1\text{mm})$ cranially.

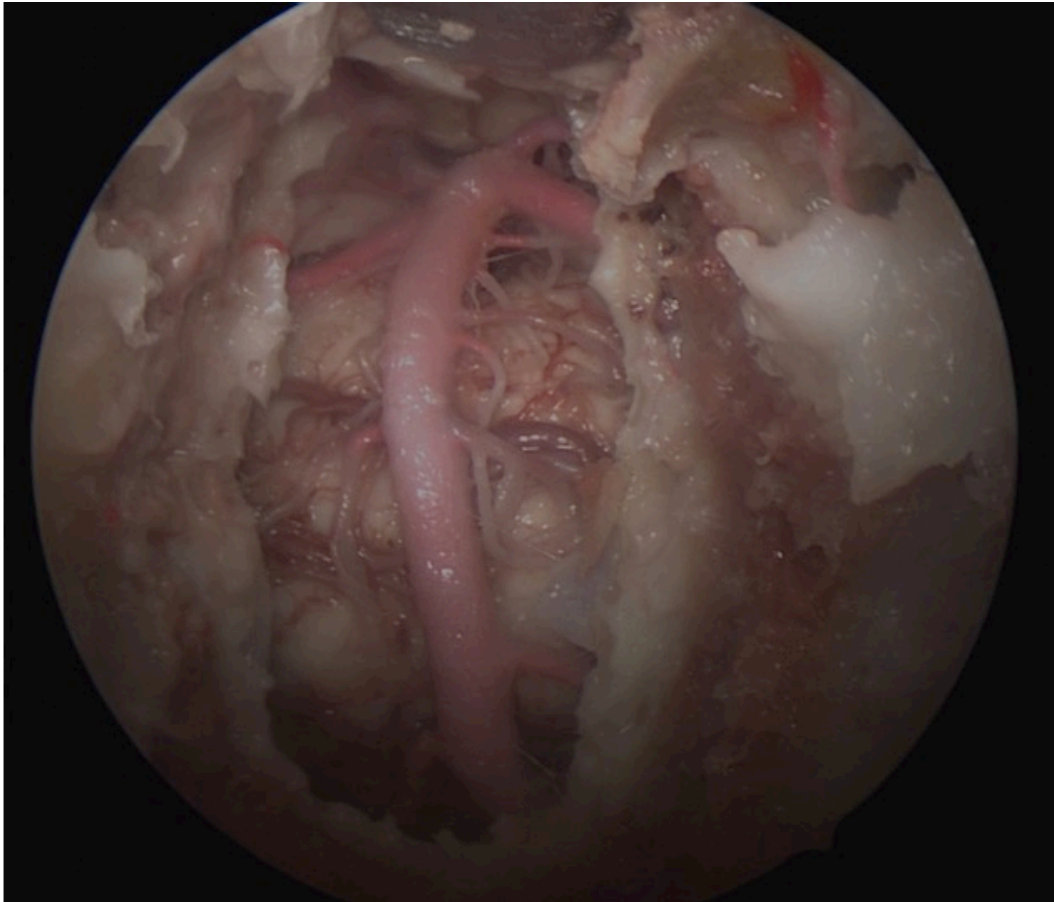


Figure 13. 3D anatomical model of the CVJ as seen from a postero-lateral perspective. Bony relationships with the main artero-venous structures are shown, i.e. with the vertebral artery, internal jugular vein and internal carotid artery. The condylar part of the occipital bone and lateral masses of atlas and axis are enclosed in a red dotted rectangular area.

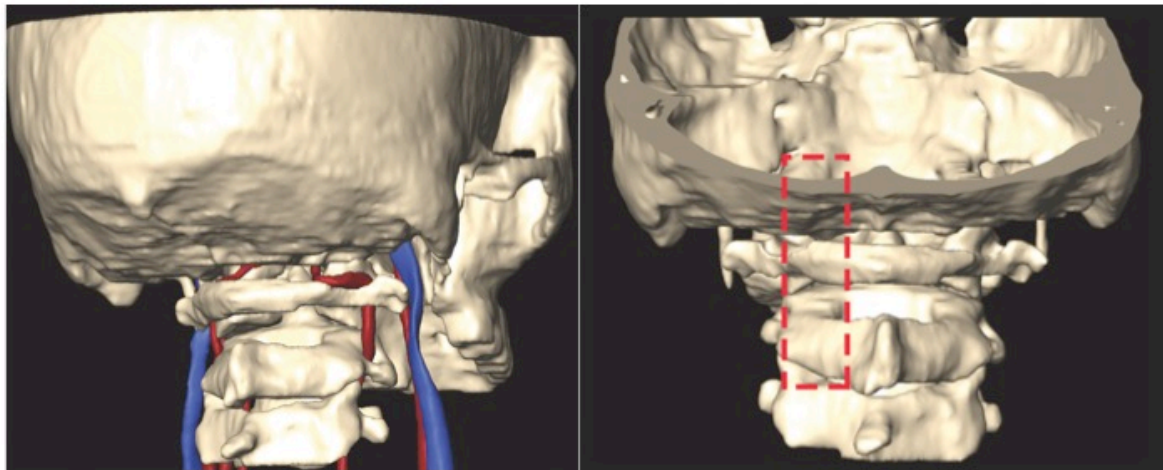


Figure 14. The segment of the vertebral artery extending from the transverse foramen of C2 to its entrance to the dura is exposed (V3). The artery, after ascending through the transverse process of the atlas, is located on the medial side of the rectus capitis lateralis muscle. From here it turns medially behind the lateral mass of the atlas and the atlanto-occipital joint and is pressed into the groove on the upper surface of the posterior arch of the atlas, where it courses in the floor of the sub-occipital triangle. EOP: external occipital protuberance; A: asterion; MP: mastoid process; V3: third segment of the vertebral artery; C1: atlas; C2: axis;

C3: third cervical vertebra; LM: lateral mass of the atlas; C1n: suboccipital nerve; C2n: second cervical nerve; C3n: third cervical nerve

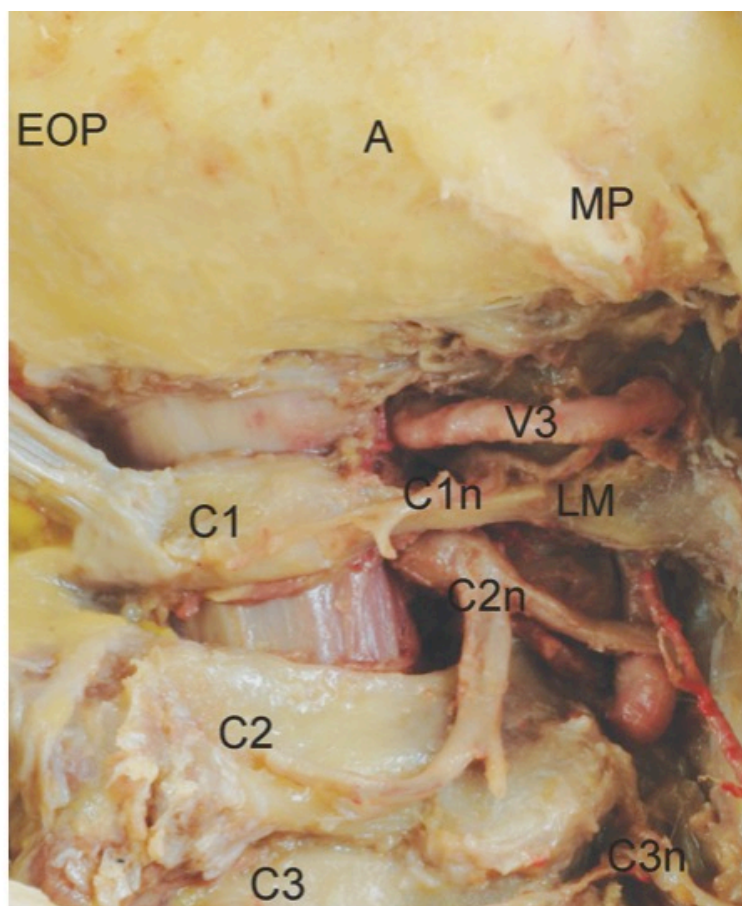


Figure 15. The muscles bounding the sub-occipital triangle are exposed and reconstructed in a 3D model on the left of the picture. The superior oblique muscle extends between the superior and inferior nuchal lines to the transverse process of the atlas. The inferior oblique muscle extends from the spinous process of the axis to the transverse process of the atlas. The rectus capitis posterior major extends from and below the lateral part of the inferior nuchal line to the spine of the axis. The triangle deep to these muscles is covered by a layer of dense fibrofatty tissue. The structures in the triangle are the V3 segment of the vertebral artery on the posterior arch of the atlas and the first cervical nerve. EOP: external occipital protuberance; A: asterion; MP: mastoid process; OA: occipital artery; IOM: inferior oblique muscle; SOM: superior oblique muscle; SCM: sternocleidomastoid muscle; RCPM: rectus capitis posterior major muscle; RCPm: rectus capitis posterior minor muscle.

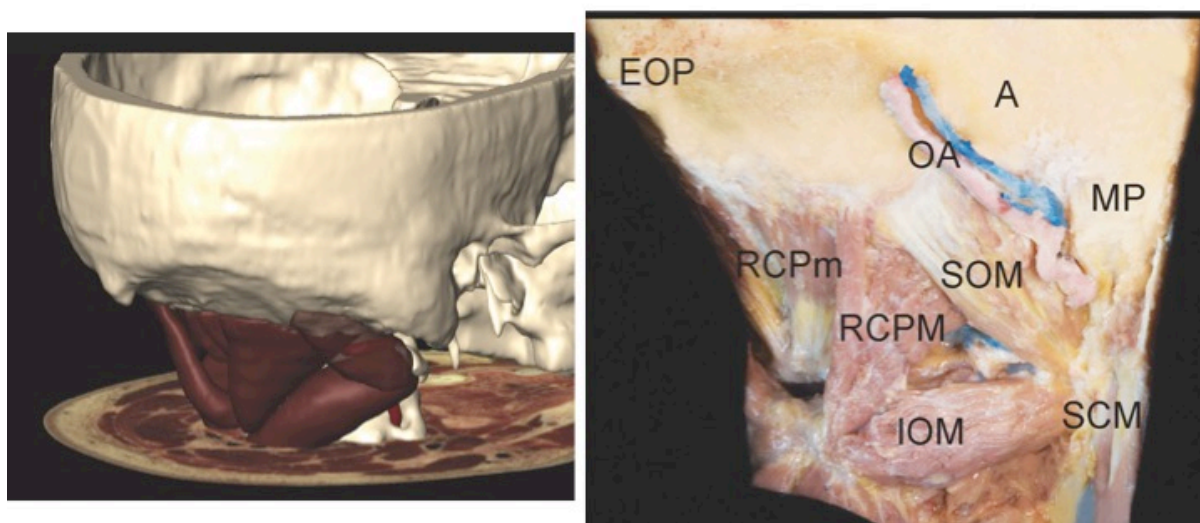


Figure 16. The intra-dural segment of the vertebral artery (V4) exposed through a postero-lateral approach can be divided in a lateral medullary segment and an anterior medullary segment. The V4 lateral medullary segment begins at the dural foramen and passes anterior and superior along the lateral medullary surface to terminate at the pre-olivary sulcus (A). The posterior inferior cerebellar artery (PICA) enters this cistern after originating from the fourth segment (V4) of the vertebral artery intra-durally. In the cerebello-medullary cistern the PICA passes dorsally between the rootlets of the IX, X and XI cranial nerve and pursue a posterior course around the medulla (B). CH: cerebellar hemisphere; T: tonsil; FM: posterior border of foramen magnum partially opened; C1: atlas partially removed; PICA: posterior inferior cerebellar artery; C3: third cervical nerve; C2: second cervical nerve; D: dura mater opened; DL: dentate ligament; XI: accessory nerve; SC: spinal cord; XII: hypoglossal nerve; HC: hypoglossal canal; V4lms: lateral medullary segment of the fourth segment of the vertebral artery; IX-X: glossopharyngeal and vagal nerves.

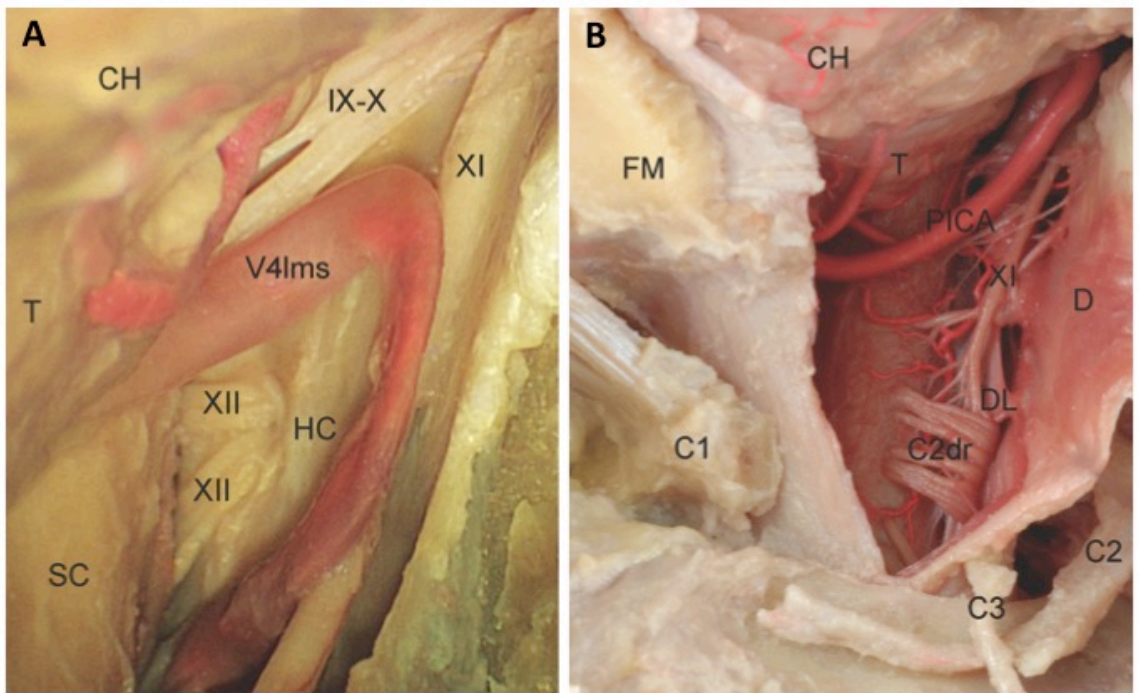


Figure 17. The antero-medial perspective of the CVJ is represented by 3D models. The area of interest after removal of the anterior arch of C1 is limited by a red dotted rectangular area on the right of the picture.

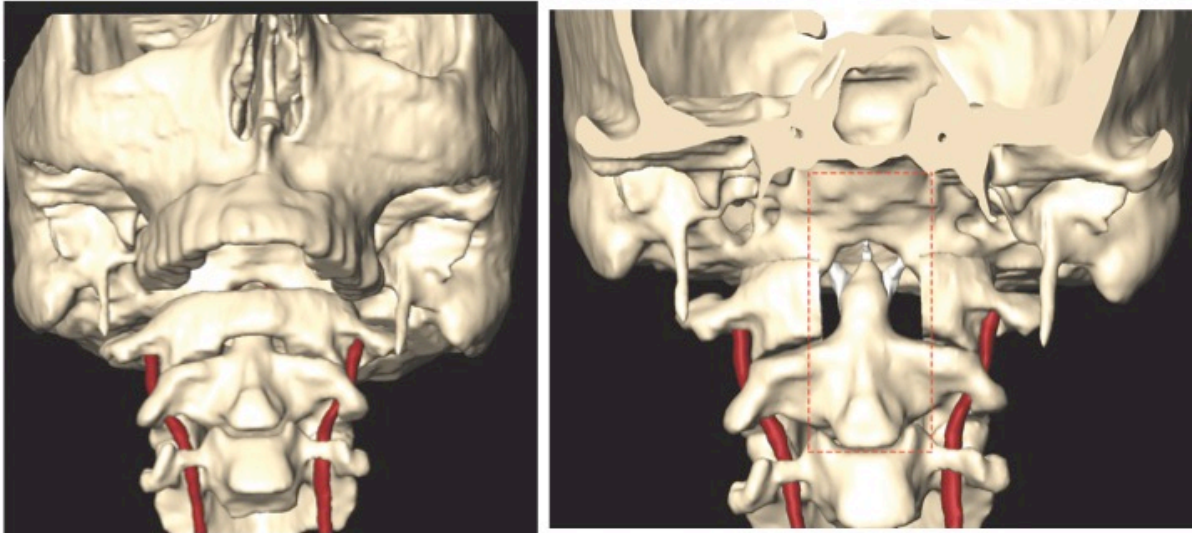


Figure 18. The fourth segment of the vertebral artery (V4) in its anterior medullary segment is visible. This segment begins at the pre-olivary sulcus, courses in front of, or between, the hypoglossal rootlets, and crosses the pyramid to join with the other vertebral artery at or near the ponto-medullary sulcus to form the basilar artery. The anterior spinal artery is formed by the union of the paired anterior ventral spinal arteries near the origin of the basilar artery. The artery descends through the foramen magnum on the anterior surface of the medulla and the spinal cord in or near the antero-median fissure. The rootlets forming the hypoglossal nerve, the glossopharyngeal, and vagal nerve run laterally from the lateral surface of the brainstem in the cerebello-medullary cistern. VAams: vertebral artery anterior medullary segment; ASA: anterior spinal artery; MPr: right medullary pyramid; MPI: left medullary pyramid; AMS: anterior median sulcus; X: vagal nerve; IX: glossopharyngeal nerve; XII: hypoglossal nerve.

